Journal of South American Earth Sciences 134 (2024) 104745

Contents lists available at ScienceDirect

Journal of South American Earth Sciences

journal homepage: www.elsevier.com/locate/jsames

Revisiting the Holocene tephrochronology of northwestern Argentina: Insights from geochemical characterization of the tephras from the Tafí valley

W. Báez [a,*], L. Bardelli [a], M.M. Sampietro-Vattuone [b], J.L. Peña Monné [c], E. Bertea [a], M. Cirer [a]

[a] Instituto de Bio y Geociencias del NOA (IBIGEO, UNSa-CONICET), Av. 9 de Julio 14, A4405BBA, Salta, Argentina
[b] Laboratorio de Geoarqueología, Facultad de Ciencias Naturales e Instituto Miguel Lillo, Universidad Nacional de Tucumán, San Miguel de Tucumán, Tucumán, Argentina
[c] Departamento de Geografía y Ordenación del Territorio and IUCA, Universidad de Zaragoza, Zaragoza, Spain

ARTICLE INFO

Keywords:
Holocene
Tephrochronology
Central Andes
Volcanic hazard
Geomorphology

ABSTRACT

In the southernmost sector of the Central Volcanic Zone (CVZ), spanning from 23° to 28°S, there is an estimated count of 30–40 potentially active volcanoes. Due to its remote location, the primary volcanic threat in this area during explosive eruptions is the dispersal and fallout of tephra. Among various approaches, tephrochronological studies have proven to be the most effective in compiling a comprehensive record of recent explosive eruptions in this region. The intermontane valleys nestled at the eastern foothills of the Andes, situated around 200–300 km from the volcanic arc, harbor a Holocene stratigraphic record containing multiple layers of tephra. These layers are evidence of the recurrence of substantial volcanic eruptions (VEI ≥4) during recent times, particularly within the last 10,000 years. Improving the tephrochronological knowledge of the southernmost edge of the CVZ constitutes a crucial initial step in evaluating the ash-fall hazard of this region. In this context, the Tafí valley emerges as a prominent candidate for serving as a dependable tephrochronological "anchor point" for regional correlations. Its strength lies in its conspicuous record of Holocene tephras and its well-documented morpho-stratigraphic setting, which has been rigorously constrained by absolute age dating. Despite these advantages, some of the Holocene tephras found within Tafí valley remain uncharacterized in terms of both glass shard and mineral geochemistry. This limitation has consequently hindered their utility in facilitating regional correlations. Thus, we present the glass shard and mineral composition of these uncharacterized Holocene tephras previously identified within Tafí valley. Our findings have not only enhanced regional correlations beyond the Tafí valley but have also provided more precise source constraints. Ultimately, our work represents an upgrade of the Holocene tephrochronological framework of Northwestern Argentina and a stride toward a more reliable assessment of volcanic hazard and risk within the region.

1. Introduction

Volcanic eruptions produce a wide range of threats, including pyroclastic density currents, lahars, volcanic edifice collapses, lava flows, and ballistic block impacts (Hansell et al., 2006). However, tephra dispersion by volcanic plumes is the only volcanic processes with the capacity to massively affect people and infrastructures over large areas, even on a continental scale, impacting multiple countries simultaneously (e.g. Donovan et al., 2023). Recent eruptions have demonstrated that, while the dispersion and deposition of volcanic tephra rarely result in fatalities, the resulting economic and environmental consequences encompass substantial threats to public health, disruption of vital infrastructure services, aviation, and various forms of production, notably agriculture and livestock (Jenkins et al., 2015). These disturbances manifest in the short, medium, and long term, rendering the hazard and risk assessment of this phenomenon a challenging task, even considering small eruptions (e.g., Forte et al., 2022). A crucial first step in assessing the ash-fall hazard of a region is to have a comprehensive inventory of recent explosive eruptions (including accurate age determination and eruptive parameters) in order to estimate the recurrence rates and magnitudes of these events (e.g., Shane and Hoverd, 2002; Hurst and Smith, 2004, 2010; Jenkins et al., 2007; Turner et al.,

* Corresponding author.
E-mail address: geowbsalta@gmail.com (W. Báez).

https://doi.org/10.1016/j.jsames.2023.104745
Received 6 September 2023; Received in revised form 11 December 2023; Accepted 12 December 2023
Available online 19 December 2023

2008, 2009; Lindsay et al., 2009). Systematic tephrochronological studies represent the most effective approach to achieve a comprehensive record of explosive volcanism within a specific volcanic center or region (Lowe, 2011). Tephra sequences preserved in various sedimentary environments (e.g., peats, marine or lake sediments, ice, etc.) at medial and distal distances generally offer more comprehensive records compared to those in proximity to the source (Lowe, 2011). This is due to the intricate stratigraphy characterizing proximal zones, which results from the superposition of numerous constructive and destructive processes associated with volcanic activity. Tephra characterization and correlation achieved through a multi-proxy approach is a fundamental basis for determining the recurrence rate of explosive eruptions within a specific region (Lowe, 2011). High-resolution tephra characterization includes glass shard morphology, mineral assemblages, major and trace elements of both glass and minerals, absolute ages, as well as considerations about the stratigraphy, geomorphology, and archaeological context.

From the Upper Eocene-Lower Oligocene to the present, the Central Volcanic Zone (CVZ, Fig. 1a) of the Andes (14–28°S) has been characterized by a prolific arc volcanism featuring hundreds of stratovolcanoes, collapse calderas, dome complexes, and mafic monogenetic centers (e.g., Trumbull et al., 2006; Kay y Coira 2009; Guzmán et al., 2014; Petrinovic et al., 2017; Wörner et al., 2018; Bertin et al., 2022, 2023; Báez et al., 2023). In the southernmost sector of the CVZ (23-28°S), there are an estimated 30 to 40 volcanoes that are considered as potentially active (de Silva y Francis, 1991; Lara et al., 2011; Amigo et al., 2012; Elissondo et al., 2017; Aguilera et al., 2022; Bertin et al., 2022). These active arc and rear-arc volcanoes lay along the Chile-Argentina border, and most of them are far from populated urban centers. Therefore, the tephra dispersion and fallout during explosive eruptions (especially with VEI $\geq$4) constitute the main volcanic threat in this region. This is especially true for the Argentine territory, where the influence of the western subtropical jet in the middle and upper troposphere (Garreaud et al., 2009) tends to disperse the tephras to the east.

Unlike the Southern Volcanic Zone (SVZ), which has recorded dozens of historic eruptions from several volcanoes (Dzierma and Wehrmann, 2012), in the southernmost sector of the CVZ, only the Lascar volcano records confirmed historical explosive eruptions (Gardeweg et al., 1998). However, it should be considered that most of the volcanoes in this region have little or no information about their eruptive history, especially for the Holocene (Bertin et al., 2022). In contrast, Holocene stratigraphic record along the intermontane valleys located at the eastern foothills of the Andes (200–300 km from the arc, Fig. 1b) includes several tephra layers revealing the recurrence in Holocene times (<10Ka) of large volcanic eruptions (Strecker, 1987; Malamud et al., 1996; Bolli, 1996 Hermanns et al., 2000; Hermanns and Schellenberger, 2008; Hain et al., 2011; Sola et al., 2016, 2018; Sampietro-Vattuone et al., 2016, 2017, 2018a,b, 2020a,b; Retamoso et al., 2021; Fernández Turiel et al., 2019). Some of these tephras were correlated with the Cerro Blanco Volcanic Complex (CBVC, Fig. 1b), the site of one of the largest Holocene eruptions in the Central Andes, which 4200 years ago blanketed the northwestern Argentina with a thick layer of ash and significantly impacted the local human inhabitation (Montero López et al., 2009; Ratto, 2013; Báez et al., 2015, 2020a,b; Fernández-Turiel et al., 2019; Sampietro-Vattuone et al., 2020a; Boretto et al., 2021; Carbonelli et al., 2022). However, up to now, there has been no comprehensive tephrochronology study of the Holocene tephras distributed in this region. For instance, the Tafí valley is an intermontane depression located ~250 km eastward from the main arc (Fig. 1c), which has a superb knowing of its Holocene morpho-stratigraphic setting, including a general physicochemical and geochronological characterization of the complete set of Holocene tephras (Peña Monné and Sampietro Vattuone, 2016; Sampietro-Vattuone and Peña-Monné, 2016, 2019; Sampietro Vattuone et al., 2016, 2018a, 2020a). However, the unequivocal regional correlation of these tephras and the identification of their sources represent a controversial issue (e.g. Fernández-Turiel et al., 2019).

This paper presents a geochemical characterization of glass shards and minerals (major elements composition) of the Holocene tephras (previously defined by Sampietro Vattuone et al., 2020a) cropping out in the Tafí valley. Our results have enabled us to enhance its regional correlation beyond the Tafí valley and to better constrain their sources. Finally, our findings constitute a valuable upgrade of the Holocene tephrochronological setting of NW Argentina and represent a step forward in achieving a reliable volcanic hazard and risk assessment for this region.

2. Geological setting

2.1. Tafí valley

The Tafí valley (Fig. 1b and c) is a tectonic depression located in the northern Sierras Pampeanas (NW Argentina), about 250 km eastward of the main volcanic arc, bordered by the Aconquija (4600 m) and the Cumbres Calchaquíes (4177 m) ranges. Both ranges are composed by Precambrian–Lower Paleozoic igneous and metamorphic rocks along with Paleogene continental deposits (Ruiz Huidobro, 1972; Toselli et al., 1978; Galván, 1981; González, 1997). The Tafí tectonic depression exposes a mainly Holocene infill (e.g., Sampietro-Vattuone and Peña-Monné, 2019), although scattered outcrops of Pleistocene loess also exist (Collantes, 2007). The Holocene stratigraphy of the Tafí valley is divided into four Holocene aggradation units separated by incision phases (Fig. 1c. Peña Monné and Sampietro Vattuone, 2016; Sampietro-Vattuone and Peña- Monné, 2016, 2019; Sampietro Vattuone et al., 2016, 2018a). The oldest unit (H1) consists of slope deposits accumulated during the Lower-Middle Holocene (*ca.* 13000 to 4200 yr BP) in a humid environment that progressively transitioned to drier conditions. During the Upper Holocene, the accumulative units H2 (*ca.* 4200 and 600 yr BP) and H3–H4 (*ca.* 600 yr PB to the present time) were deposited. The H2 units is constituted by slopes, alluvial terraces, and alluvial fan deposits. The H2 units recorded paleosoils formation under wetter conditions. One outstanding feature of the H2 units is the evidence of soil degradation caused by human activity (Sampietro Vattuone et al., 2018b; Peña-Monné and Sampietro-Vattuone, 2019). Finally, smaller deposits forming the H3 and H4 units occur along the main incisions that crosscut the preceding aggradational units. These units were deposited during the Little Ice Age and the current warm period.

2.2. Holocene tephrochronology of the NW Argentina

Despite the conspicuous Cenozoic volcanism along the southern edge of the CVZ (23-28°S), tephrochronological studies in this region have been limited thus far (e.g., Hermanns and Schellenberger, 2008; Coira et al., 2014, 2022a, b; Fernández-Turiel et al., 2019; Sampietro Vattuone et al., 2020a). On the other hand, some studies used tephra layers to establish a temporal framework for various geological processes, such as sedimentation rates during basin infilling, recurrence and triggering factors of rock avalanches, or paleoenvironmental reconstructions (e.g., Malamud et al., 1996; Hermanns et al., 2000; Trauth et al., 2003; Hain et al., 2011; Guerra et al., 2022; Sampietro Vattuone et al., 2020b).

Specifically for the Holocene, despite the early mentions (e.g., Frenguelli, 1936), Malamud et al. (1996) provided the first absolute age constraint for a <10 ka tephra cropping out near the top of the La Viña Formation in the Lerma valley (Fig. 1b). This work presented radiocarbon ages of carbonaceous silts and charcoal that encompass a tephra layer ("ash C″), constraining its age to 3700–5400 years BP. Later works covering a wider region (Lerma, Calchaquí, Santa María and El Tonco valleys, among others. Fig. 1b) expanded the catalog of Holocene tephras defining the "Cerro Paranilla"(>7820 ± 830 yr. BP.), "El Paso" (>7430–7570 and < 10580–11150 yr. BP.), "Buey Muerto"(>3930–4410 and <4520–4960 yr. BP.), "Alemanía" (<3470–3830 yr. BP.), and "Villa Vil" (~980–1540 yr. BP.) ashes

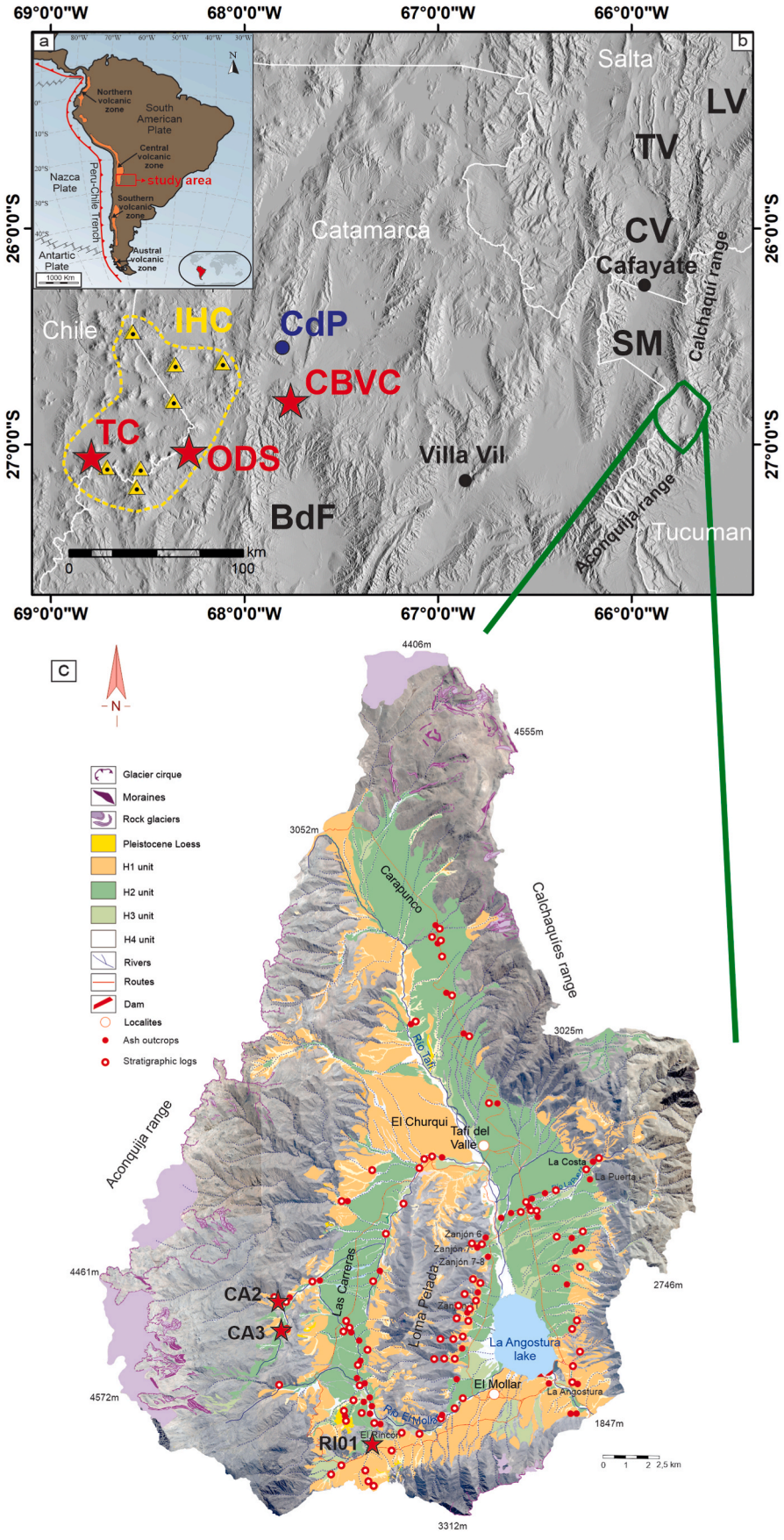

(caption on next page)

Fig. 1. a) Location of the Central Volcanic Zone (CVZ) in the geodynamic framework of South America. b) Location of the volcanic centers, localities, ranges and intermontane valleys mentioned in the text. IHC: Incahuasi volcanic cluster; TC: Nevado Tres Cruces volcano; ODS: Ojos del Salado volcano; CBVC: Cerro Blanco Volcanic Complex; CdP: Cueros de Purulla volcano; BdF: Bolsón de Fiambala valley; SM: Santa María valley; CV: Calchaquí valley; TV: Tonco valley; LV: Lerma valley. Green polygon indicates the location of Tafí valley. c) Morpho-stratigraphic map of the Tafí valley (after Sampietro-Vattuone and *Peña-Monné, 2019*). Red circles mark the localities that record Holocene tephras and the red stars the three localities discussed in this work.

(Hermanns et al., 2000; Hermanns and Schellenberger, 2008). The Villa Vil ash, which crops out in the homonymous locality (Fig. 1b), represents the first evidence of the occurrence of a large explosive eruption during the Upper Holocene. These studies represent the initial attempt to provide a systematic Holocene tephrochronological framework on a regional scale (NW Argentina), including identification of physical-chemical fingerprints and absolute-age constraints. In this context, the "ash C" (Malamud et al., 1996) was correlated to the "Buey Muerto" ash (Table 1).

However, the first work that identified the source of some of the Holocene distal tephras in NW Argentina was that of Fernández-Turiel et al. (2019). These authors applied geochemical fingerprints and carbon-14 ages to correlate distal ashes from Tafí, Santa María and Calchaquí valleys ("Cerro Blanco Sequence" hereafter "CBS") to the Holocene explosive activity of the Cerro Blanco Volcanic Complex (Table 1; Montero-López, 2009, Montero-López et al., 2010; Báez et al., 2015). Fernández-Turiel et al. (2019) claimed that the Cerro Blanco eruption occurred ~ 4200 yr. BP, representing the largest Holocene eruption in the Central Volcanic Zone of the Andes (probably one of the largest worldwide). However, some criticisms exist regarding the definition of the eruptive parameters (Báez et al., 2020a). Fernández-Turiel et al. (2019) correlated the "CBS" with the "Buey Muerto ash" (Hermanns and Schellenberger, 2008) and the "ash C" (Malamud et al., 1996). Fernández-Turiel et al. (2019) also defined another two tephra layers (Table 1), the "Cueros de Purulla Sequence" (hereafter "CdPS") and the "Bolsón de Fiambala Sequence" (hereafter "BdFS"). The "CdPS" includes geochemically well-correlated distal tephras cropping out near Cafayate (Fig. 1b) along with proximal plinian fall-out deposits and ignimbrites assigned to the Cueros de Purulla volcano (Fig. 1b. Fernández-Turiel et al., 2019; Bertea et al., 2021). The "CsPS" was assigned to the Early–Holocene by correlation with the "Cerro Paranilla ash" (Hermanns and Schellenberger, 2008). However, this correlation is weak since it is based solely on the macroscopic identification of abundant large biotite crystals in both units. The "BsFS" crops out along the homonymous valley (Fig. 1b). This unit was assigned to the Upper Holocene and likely derived from the Nevado Tres Cruces Volcanic Complex (Fig. 1b. Fernández-Turiel et al., 2019).

Finally, Sampietro Vattuone et al. (2020a) presented a tephrochronological study of the Tafí valley (Table 1; Figs. 1c and 2) identifying four Holocene tephras (V0, V1a, V1b, and V2). In such work, the four tephras were identified based on their morpho-stratigraphic position (supported by absolute ages) as well as by their overall mineralogical and geochemical (bulk) composition. Additionally, they established correlations beyond the Tafí valley by using geochronological data rather than geochemical fingerprints (Sampietro Vattuone et al., 2020a). For example, the rhyolitic V0 tephra was assigned to the Lower Holocene (<11802–11192 and >4789–4289 yr. BP) and correlated with the "El Paso ash" (Hermanns and Schellenberger, 2008) and the "CdPS" (Fernández-Turiel et al., 2019). However, there appears to be an apparent mismatch with previous correlations, as Fernández-Turiel et al. (2019) correlated the "CdPS" with the "Cerro Paranilla ash" and not with the "El Paso ash". The rhyolitic V1a (<4789–4289 and >3830–3470 yr. BP) and V1b (<3830–3470 BP and >2760–2188 yr. BP) ashes were correlated to the "Buey Muerto" and "Alemanía" respectively (Hermanns and Schellenberger, 2008). Both tephras are hard to differentiate from each other using their texture, mineralogy, as well as their geochemistry, at least considering the major elements concentrations of glass shards or the major and trace elements concentration of bulk samples (Hermanns and Schellenberger, 2008; Sampietro Vattuone et al., 2020a). In addition, both tephras have geochronological, geochemical, and mineralogical features that resemble the "CBS" (Fernández-Turiel et al., 2019). Thus, the distal ashes previously attributed to the major Cerro Blanco eruption (as defined by Fernández-Turiel et al., 2019) likely represent the occurrence of two Plinian eruptions that took place in close succession and were fed by the same magmatic system—the Cerro Blanco Volcanic Complex (Sampietro Vattuone et al., 2020a). While the presence of both V1a and V1b tephras in a single profile allows for their unequivocal identification, it becomes virtually impossible to distinguish between them when only one is exposed (Hermanns and Schellenberger, 2008; Sampietro Vattuone et al., 2020a). The dacitic V2 tephra was assigned to the Upper Holocene (younger than 800 yr. BP) and correlated with the "BdFS", thus linking it to the Tres Cruces Volcano (Fernández-Turiel et al., 2019). Some geochronological evidence from Santa María valley (Fig. 1b) suggests that the V2 tephra actually includes two independent ash layers named V2a (<991–774 and > 655–624 yr. BP) and V2b (<497–468 yr. BP), which are compositionally almost identical (Sampietro Vattuone et al., 2020a). However, a more robust and spatially extensive data set is required to confirm these observations. In summary, Sampietro Vattuone et al. (2020a) showed that the Tafí valley could be a faithful tephrochronological "anchor point" for regional correlations, as it is characterized by a well-known morpho-stratigraphic setting and by the preservation of multiple tephra layers in individual profiles. However, until now, the Holocene tephras from Tafí valley have not undergone a comprehensive geochemical characterization of their glass shards and minerals, limiting their utility for regional correlations.

Table 1
Synthesis of the Holocene tephrochronology of NW Argentina. The Upper Pleistocene (UPL) tephras are also present (see the text for its discussion). BsF: Bolsón de Fiambala Sequence; CBS: Cerro Blanco Sequence; CdPS: Cueros de Purulla Sequence; CBVC: Cerro Blanco Volcanic Complex.

	Malamud et al. (1996)			Hermanns and Schellenberger (2008)			Fernández Turiel et al. (2019)			Sampietro Vattuone et al. (2020a) and this study		
	Name	Age	Source	Name	Age	Source	Name	Age	Source	Name	Age	Source
H	X	X	X	Villa Vil	~1.4 Ka	?	BsFS	<1.5 Ka	Nevado Tres Cruces	**V2**	**~0.7 ka**	**Incahuasi cluster**
O	X	X	X	Alemanía	<3.8 Ka	?	X	X	X	**V1b**	**~3.5 Ka**	**CBVC**
L	Ash C	5.1–3.9 ka	?	Buey Muerto	3.8–4.9	?	CBS	~4.2 Ka	CBVC	**V1a**	**~4.2 Ka**	**CBVC**
O	X	X	X	El Paso	10.5–7.5 ka	?	X	X	X	**V0**	**~10 Ka**	**CBVC**
C												
E												
N												
E												
UPL	Tuff B	100 ± 40 Ka	?	Cerro Paranilla	>7.8 Ka	?	CdPS	>7.8 Ka ???	Cueros de Purulla	**VP**	**~54 ka**	**CBVC**

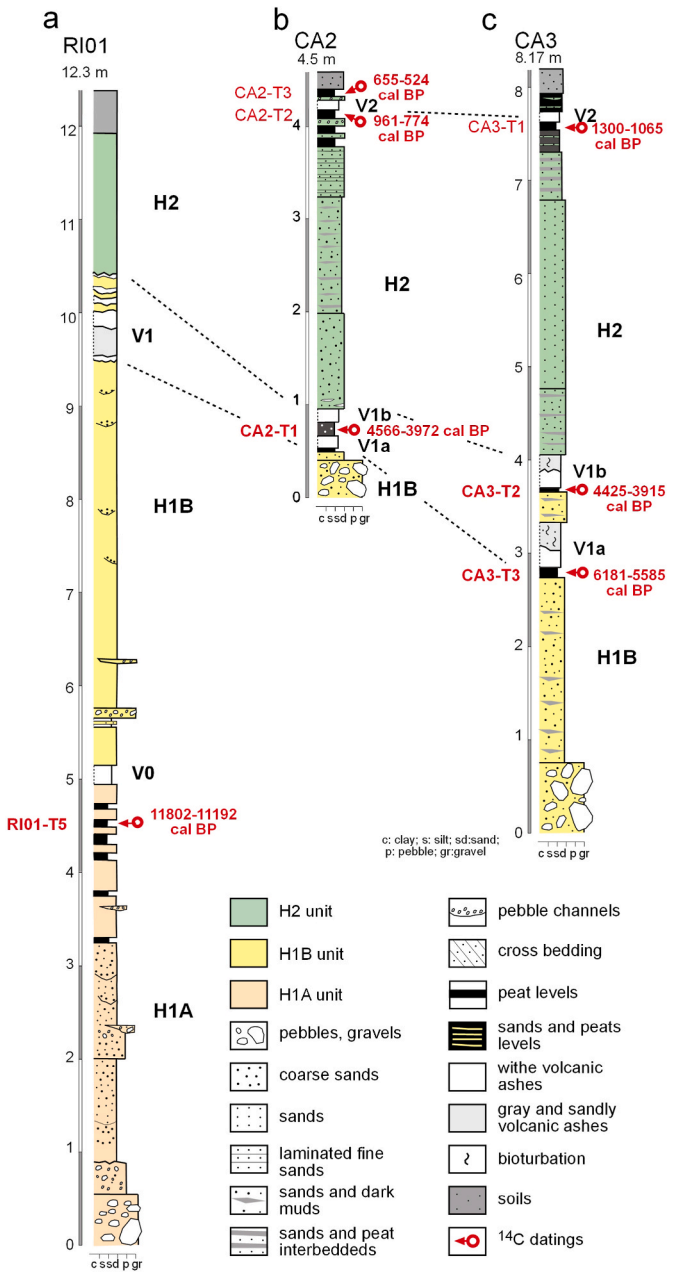

Fig. 2. Stratigraphic profiles of the three localities studied in this work: El Rincón 01 (RI01) Las Carreras 2 (CA2) and Las Carreras 3 (CA3). The morpho-stratigraphic units and the chronological data of V0, V1a, V1b, and V2 tephras are also showed (modified from Sampietro-Vattuone et al., 2020a).

3. Methodology

To refine the geochemical fingerprints of the four tephras previously identified by Sampietro Vattuone et al. (2020a) in the Tafí valley, we conducted electron probe microanalyses ("EPMA") on glass shards and minerals from five selected samples with a well-constrained chronology (Fig. 2). The selected ash deposits correspond to one sample from V0 (RI01), two samples from V1a (CA2-V1a, CA3-V1a), one sample from V1b (CA3-V1b), and two samples from V2 (CA2-V2, CA3-V2). To test the potential correlation of V0 with the Cueros de Purulla Volcano (Fernandéz-Turiel et al., 2019), we have included novel data from the proximal fallout deposits (pumice clasts identified as CDP) associated with the Cueros de Purulla Volcano (Bertea et al., 2021). We also explored other possible correlations using data from the literature (see section 5.2).

The EPMA of the considered tephras samples were carried out at the LAMARX (*Laboratorio de Microscopía Electrónica y Análisis por Rayos X*) at the National University of Córdoba using a Jeol JXA-8230 electron microprobe. For samples CA2-V1a, CA3-V1a, CA3-V1b, CA2-V2, and CA3-V2, the <2φ fraction was separated by manual sieving and then mounted on uncovered thin sections. EPMA of sample CDP was conducted on an uncovered thin section of an individual pumice clast. The EPMA concerned the measurement of elements such Si, Ti, Al, Fe, Mn, Mg, Ca, Na, K, P, F, and Cl for samples (n = 5) selected by petrographic observations. We analyze all mineral phases except for quartz, some iron-titanium oxides, and apatite, which are present as accessories. Current and voltage conditions were set at 10 nA and 20 kV respectively, with a beam size of 10 and 5 μm for minerals and glass, respectively. The counting time for silicate minerals was of 20 s, and the elements F and Na were considered first to reduce the loss during the measurement. For the considered elements, errors are in the range 0.13–0.85 %, except for F that is associated to an error of 2.15 %. A set of reference materials (i.e., natural and synthetic standards) was used for routine calibration and instrument stability monitoring, during the analytical session. The Fe content was reported as total FeO. Repeated analyses of the standards resulted in one-sigma (1σ) precision (i) better than 1.5% for Si; (ii) better than 2% for Al; (iii) better than 5% for other oxides and F. Detection limits resulted in 0.10 wt% for SiO_2 and 0.04 wt% for the other oxides. All mineral analyses showing anomalous lower totals or closure higher than 101 wt% were excluded. Validation of mineral chemistry results was achieved through opportune comparisons with the existing literature, following the method and the references proposed in Lucci et al. (2020).

4. Results

We present in this section the representative results obtained by the EPMA study for the volcanic glass and the main mineral phases (plagioclase, K-feldspar, biotite, amphibole). The glass analyses are normalized on a 100% anhydrous base before interpreting the results. The entire chemical dataset obtained in this study is provided in the Supplementary Table S1, and the representative textures and mineral assemblage of each tephra are presented in Fig. 3. The V0 tephra has a mineral assemblage dominated by plagioclase, quartz, and K-feldspar (in order of abundance). Additionally, the V0 tephra is characterized by relatively abundant mafic minerals, mainly biotite ± amphibole. Accessory phases include iron oxides, titanite, and apatite. The V1a and V1b tephras have a mineral assemblage dominated by plagioclase, quartz, and K-feldspar (in order of abundance). However, they differ from the V0 tephra by their low percentage of mafic minerals, mainly biotite. Iron oxides are also present as an accessory phase. The V2 tephra has a mineral assemblage dominated by plagioclase, amphibole, and biotite ± quartz. The amphibole-rich composition of the V2 tephra represents its main petrographic fingerprint. Accessory phases include iron oxides and apatite.

In general, the observed mineral assemblage aligns with prior studies (Sampietro Vattuone et al., 2020a), with the notable exception of the occurrence of subordinate amphibole alongside biotite in the V0 tephra layer (Fig. 3). Such differences may be attributed to the analysis of different grain size fractions, as Sampietro Vattuone et al. (2020a) used fraction with sizes greater than 2φ.

4.1. Glass

The analyses concerned vesiculated fragments of volcanic glass generally smaller than 150 μm. The obtained SiO_2 contents range ca. 76–79 wt %, with just one analyses (sample *CA2-V2*) showing 73.6 wt % SiO_2 (Supp. Table S1). A rhyolitic composition ($Na_2O + K_2O$ = 7.5–8.7 wt %) and a high-K calc-alkaline character (K_2O = 4.2–5.1 wt %) distinguish all the analyzed glass spots (Fig. 4a and b), which are also

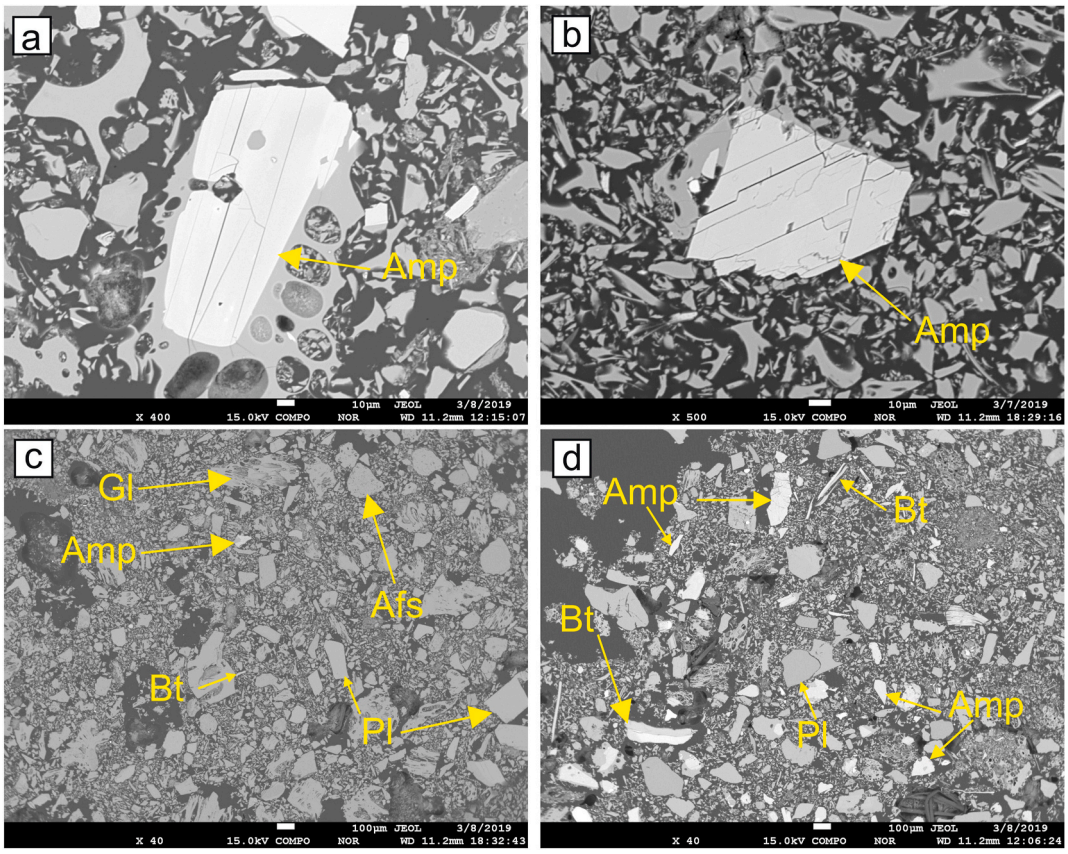

Fig. 3. Representative mineral assemblage of the analyzed ash samples represented by back-scattered electron images ("BSE"). a-b) Examples of the previously unreported amphibole crystals of the sample RI01-V0. c) General texture of the V1b tephra (sample CA3-V1b) showing its low percentage of mafic minerals (mainly biotite). The V1a tephra (not showed) presents almost identical textural features as V1b. d) General texture of the V2 tephra (sample CA3-V2) showing its amphibole-rich composition. Scale bar is of 10 µm for Fig. 3a and b, and of 100 µm for Fig. 3c and d.

characterized by peraluminous affinity (Fig. 4c). A general pattern of evolution in glass composition is evident when considering the progressive increase in the SiO_2 content from V2 (less evolved) to V1b (more evolved), and passing successively through V0 and V1a (Fig. 4a and b). The inter-sample distribution of the other mayor oxides indicates homogeneous compositions (Fig. 4d–f. Supp. Table S1). As an exception to that, the *V2* ash samples display the highest CaO (up to ca. 1.5 wt %) and FeO (up to 1.6 wt %) contents.

4.2. Feldspars

The feldspar families recognized in the studied ash samples consist of plagioclase with oligoclase to labradorite composition (X_{An} 0.14–0.61, being X_{An} the anorthite fraction) and by sanidine (X_{Or} 0.26–0.77, being X_{Or} the orthoclase fraction; Fig. 5a). The plagioclase crystals from samples *V0* are predominantly andesine (X_{An} 0.26–0.36) and are associated with K-feldspar crystals with X_{Or} of 0.75–0.77. In the samples *V1*, plagioclase is oligoclase and andesine (X_{An} 0.15–35) and, apparently, two populations of sanidine are present in association (X_{Or} 0.41–0.44 and X_{Or} 0.68–0.74, respectively). The most anorthite-rich plagioclase crystals are recognized within the *V2* ash and *CDP* pumice samples (X_{An} up to 0.50 and 0.61, respectively), and the highest FeO contents (up to 0.7 wt%) characterize the sample *CA3-V2* (Fig. 3e). Conversely, plagioclase crystals in the sample *CA3-V1b* display the lowest Al_2O_3 contents (ca. 18–20 wt %; Fig. 5b).

4.3. Biotite

Dark trioctahedral biotite crystals are present in all the analyzed ash samples (according to Rieder et al., 1998; cationic contents calculated following Li et al., 2020). These crystals are characterized by wide ranges of TiO_2 and a narrower range of MnO, except for the sample *CA3-V1b* (Fig. 5c and d). In addition, the studied samples display a broad spectrum of cationic Ti (0.15–0.32 apfu), $Al^{[iv]}$ (0.86–1.25 apfu) and Fe# [0.26–0.53, being Fe# the $Fe^{2+}/(Fe^{2+}+Mg)$ cationic ratio]. The most Al-rich crystals (Al_2O_3 up to 19 wt%) belong to the sample *CA2-V1a* and are also associated to high CaO (up to 0.4 wt%) and low MgO (ca. 9–10 wt%) contents (Supp. Table S1). Samples *CA3-V2* and *CDP* are enriched in titanium (TiO_2 up to ca. 6.0 wt%), whereas samples *CA2-V1a* are enriched in $Al^{[iv]}$ (up to 1.25 apfu) and relatively depleted in Ti (<2.0 apfu; Fig. 5d).

4.4. Amphibole

Amphibole is a widespread mineral phase in the analyzed ash samples. According to Ridolfi et al. (2018), they belong to the W (OH–F–Cl)-dominant group, Ca sub-group (n = 37). According to Locock (2014), these amphibole crystals classify as magnesio-hornblende (n = 8), magnesio-ferri-hornblende (n = 10), ferro-hornblende (n = 1), magnesio-hastingite (n = 5), hastingite (n = 1), Ti-rich magnesio-hastingite (n = 1), pargasite (n = 8), Ti-rich pargasite (n = 1), and actinolite (n = 1). Similarly to what observed for the biotite, the analyzed amphibole crystals display wide compositional ranges, particularly considering the cationic Ti (ca. 0–0.36-apfu), the tetrahedral $Al^{[iv]}$ (0.6–1.8 apfu), and Mg# (0.47–0.75). Amphibole crystals from samples *V2* are enriched in TiO_2 (1.2–3.3 wt%; Table S1e) and Mg (0.63–0.75 Mg#), whereas the crystals from sample *CA3-V1b* are depleted in these elements (0.3–1.6 TiO_2, and 0.47–0.68 Mg#) at similar $Al^{[iv]}$ contents

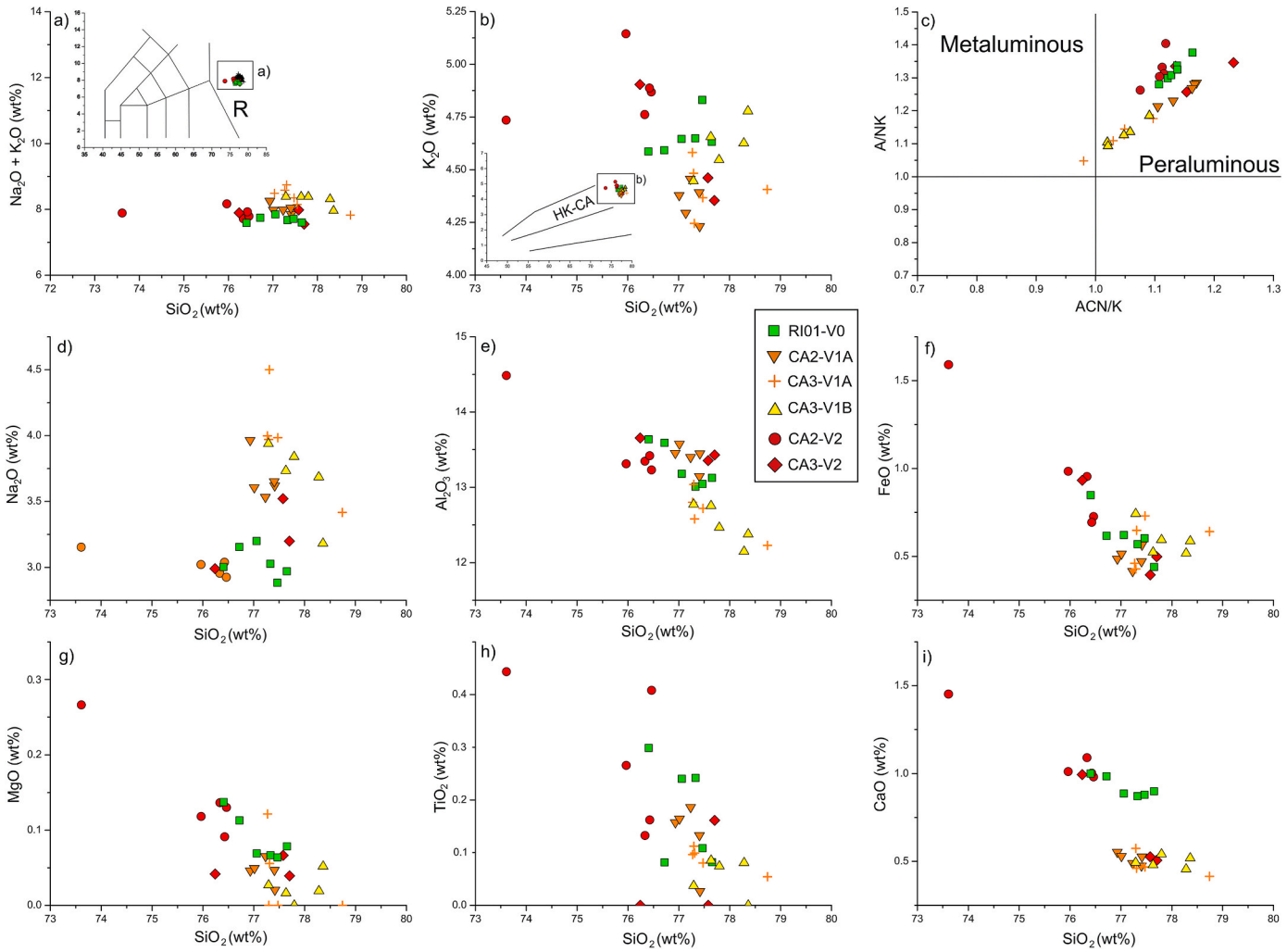

Fig. 4. Representative composition of volcanic glass of the analyzed ash samples as obtained through EPMA study. a) TAS (total alkali versus silica) diagram (R = rhyolitic field). b) K2O versus SiO2 (after Peccerillo and Taylor, 1976). HK-CA = high-K calc-alkaline field. c) ASI (alumina saturation index) with A/CNK (molar Al2O3/CaO + Na2O + K2O) versus A/NK (molar Al2O3/Na2O + K2O). d-i) Harker diagrams with SiO2 used as differentiation index for Na2O, Al2O3, FeO, MgO, TiO2 and CaO.

(Fig. 5e and f). Considering the alumina number [Al# = $Al^{[vi]}/(Al^{[vi]}+Al^{[iv]})$] as a discriminant between possible phenocryst (Al# < 0.21) and xenocrysts (Al# > 0.21) (following Ridolfi et al., 2010), it can be observed in Fig. 5e how the analyzed amphibole crystals of the samples CA2-V1a and CA3-V1b fall in the xenocrystic field. We did not observe amphibole crystals in the pumice sample *CDP*.

5. Discussions

5.1. Reliability of the geochemical fingerprints of the tephras from the Taff valley

To identify distinctive fingerprints of the studied tephras, we discuss the results of our EPMA analysis in the following paragraph. In general, the full characterization and unequivocal identification of each tephra requires a multi-proxy approach.

The glass composition (major elements) shows considerable overlapping in most of the diagrams (Fig. 4). However, the four tephras can be separated in the K_2O vs SiO_2 plot. The V2 tephra has a less evolved glass composition and higher K_2O content. The V0, V1a, and V1b tephras have a more evolved glass composition, although V1a and V1b tend to have higher SiO_2 content. The K_2O values appear to be a proxy for separating V1a and V1b, although in the rest of the Harker diagrams, these differences are not maintained systematically. Additionally, the CaO vs SiO_2 diagram appears to be useful for separating V2 and V0 from V1a and V1b (Fig. 4b and i).

With respect to feldspars, the plagioclase composition of V2 and V0 overlaps (mainly andesine composition, Fig. 5a). However, the presence of sanidine in the V0 tephra allows for its differentiation from V2 (Fig. 5a). In addition, we highlight that the sanidine from the V0 tephra have a very distinctive composition (XOr 0.75–0.77; Fig. 5a). On the other hand, the plagioclases of V1a and V1b reach a more albitic composition (Oligoclase), clearly distinguishing them from V0 and V2 (Fig. 5a). The K-feldspars in V1a and V1b also differ from those in V0 (Fig. 5a). We also note that the Al_2O_3 content in the plagioclases appears to be a proxy for separating the V1a and V1b tephras (Fig. 5b).

Biotite is the most abundant mafic mineral in the V0, V1a and V1b tephras (especially in the V0 tephra), so a priori makes them a good target to discriminate among these tephras. However, our results show that the biotite composition is very similar in the four tephras studied (Fig. 5c and d). Only our CDP sample appears to have a well-defined biotite composition (Fig. 5d), and we discuss the importance of this observation in section 5.2. There are slight differences in the composition of the biotite in V1a and V1b tephras (Fig. 5c and d) that could potentially help in their identification.

Finally, amphiboles seem a very useful proxy to separate the V2 and

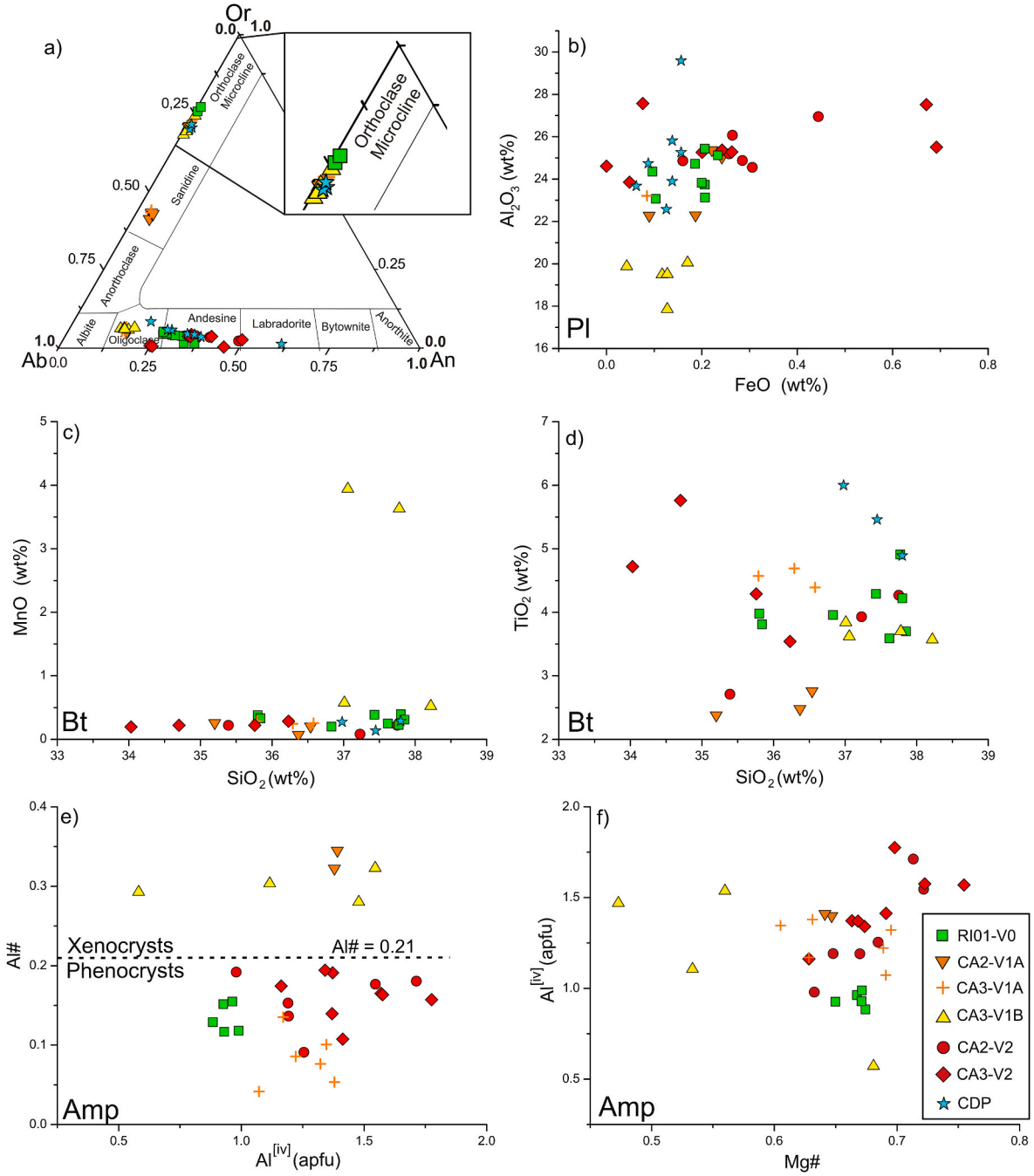

Fig. 5. Representative composition of the main mineral phases observed in the analyzed ash samples. a) Feldspar ternary diagram (anorthite-albite-orthoclase). b) Binary diagram of Al2O3 versus FeO for the plagioclase. c) Binary diagram of MnO versus SiO2 and (d) TiO2 versus SiO2 for the biotite. e) Binary diagram of the alumina number (Al# = Al[vi]/Al[vi]+Al[iv]; following Ridolfi et al., 2010) versus Al[iv] (apfu) for the amphibole. f) Binary diagram of Al[iv] (apfu) versus Mg# [being Mg# = Mg/(g + Fe2+)] for the amphibole. Pl = plagioclase; Bt = biotite; Amp = amphibole.

V0 tephras, especially when considering the Al# vs $Al^{(iv)}$ plot (Fig. 5e and f). The V2 tephra is characterized by high contents of amphibole, and the Al# vs $A^{(iv)}$ plot indicates that these crystals may represent true phenocrysts (Fig. 5e, Ridolfi et al., 2010). Amphibole crystals from V2 clearly differ from those of the V0 tephra. Despite that the amphibole in the V0 tephra is subordinate to the biotite, they have well constrained composition that suggests a phenocrystic nature (Fig. 5e, Ridolfi et al., 2010). In contrast, the composition of V1a and V1b amphiboles shows greater dispersion, and many of these likely represent xenocrysts (Fig. 5e and f, Ridolfi et al., 2010).

In summary, the Holocene tephras from Taff valley can be identified from their geochemical fingerprints. The V2 tephra is the easiest to separate due to its less evolved glass composition, the abundance of amphiboles with a well-defined composition, and the absence of sanidine. The V0 tephra is better characterized by the specific composition of sanidine and amphibole, in addition to its clustering in the K_2O vs SiO_2 diagram. The biotite composition is not different from that of V1a, V1b, and V2, but it is useful for correlating the V0 tephra beyond Taff Valley (see section 5.2). Finally, V1a and V1b are almost identical and display the most evolved glass and a very distinctive feldspars composition. We found some potential fingerprints to discriminate between the V1a and V1b tephras, including glass (K2O), plagioclase, and biotite composition. However, a more robust analytical database (increasing the number of samples and spots), including glass trace and rare-earth

elements, is needed for reliable identification of V1a and V1b tephras.

5.2. Regional tephrochronological implications

We used the glass and mineral composition obtained from the considered ash samples for a comparison and possible correlation with other volcanic tephras of the NW Argentina. We focus our regional correlation on the tephras described by Hermanns and Schellenberger (2008) and Fernandéz-Turiel et al. (2019). Our primary goal is to provide a synthesis of the current state of knowledge regarding the Holocene tephrochronology of NW Argentina (Table 1). In addition, we delve deeper into the discussion about the sources of these tephras. Regarding this matter, it is worth noting that many of the volcanoes deemed potential sources lack detailed stratigraphic, geochronological, and volcanological studies, which complicates reliable correlation with distal deposits.

We test the potential correlation of V0 with the "CdPS" and, consequently, with the Cueros de Purulla Volcano (Fernandéz-Turiel et al., 2019). We are also considering the potential correlation of the CdPS with the Campo de la Piedra Pómez eruption (CPP), which is related to the Pleistocene activity of the CBVC (Báez et al., 2015, 2020b; Bardelli et al., 2020; 2022; de Silva et al., 2022). Regarding V1a and V1b, we aim to build upon their widely accepted correlation to CBVC (Fernandéz--Turiel et al., 2019; Sampietro Vattuone et al., 2020a) by identifying the correlation of each tephra with a specific eruptive event recorded in the proximal zone (Báez et al., 2015; Bardelli et al., 2022; de Silva et al., 2022). Lastly, we assess the correlation of the V2 tephra with the "BdFS" (Fernandéz-Turiel et al., 2019) and discuss its connection with the Nevado Tres Cruces volcano.

Our results do not support the correlation of V0 with the CdPS, and thus with the Cueros de Purulla Volcano (Figs. 6 and 7). Despite their similar glass composition, the sanidine (Ab/Or ratio) and biotite (TiO_2 wt%) are quite different (Fig. 7a and c). However, the most striking difference regards the amphibole population (Fig. 7e and f). All the amphiboles from the CdPS appear to be xenocrystals and show different composition relative to those of the V0 tephra (Fig. 7e and f). The age of the V0 tephra is well-constrained in the Tafí valley, and its correlation with the El Paso ash is quite solid due to geochronological constraint (Sampietro Vattuone et al., 2020a). In contrast, the age of the V0 tephra (<11802–11192 and >4789–4289 yr. BP) is less consistent with the available absolute age (~400 Ka) for the Cueros de Purulla volcano (Siebel et al., 2001). We compared the glass composition of the El Paso ash (Hermanns and Schellenberger, 2008) with our V0 data. Despite some affinity, the geochemical correlation is not conclusive (Fig. 6). Mineral composition data for the El Paso ash are required to improve this correlation. Considering the Holocene age and the main geochemical features of the V0 tephra (rhyolitic composition, Sampietro Vattuone et al., 2020a), the strongest candidate for their source is the CBVC. There is no other volcano in the southern CVZ with a rhyolitic explosive activity during the Holocene (Bertin et al., 2022, 2023; Báez et al., 2023). However, a major explosive eruption of this age has not been clearly defined in the proximal zone of the CBVC (Báez et al., 2015; Bardelli et al., 2022; de Silva et al., 2022). Even so, some works mentioned the occurrence of several explosive eruptions in the CBVC during the Lower Holocene (Montero-López, 2009; Montero-López et al., 2010). It is necessary to improve the resolution of the CBVC

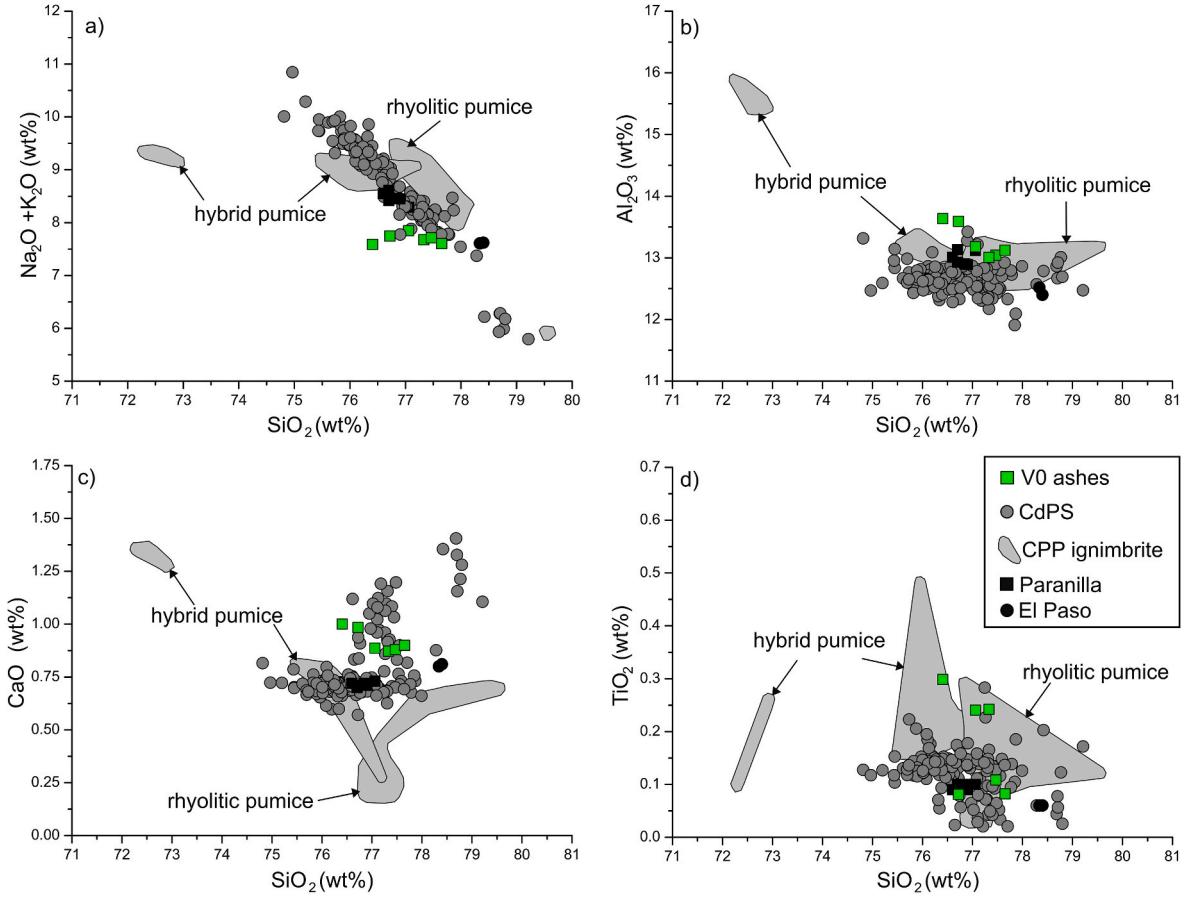

Fig. 6. Comparison of the V0 ashes with (i) the CdPS ash samples of Fernandéz-Turiel et al. (2019,and references therein), (ii) the CPP (Campo de la Piedra Pómez) ignimbrite (Bardelli et al., 2020), and (iii) the Paranilla/El Paso ash samples (average composition) following Hermanns and Schellenberger (2008). For the CPP Ignimbrite we include data from the dominant rhyolitic pumice and also from the volumetrically less important hybrid pumice (Bardelli et al., 2020). a) Na2O + K2O versus SiO2. b) Al2O3 versus SiO2. c) CaO versus SiO2. d) TiO2 versus SiO2.

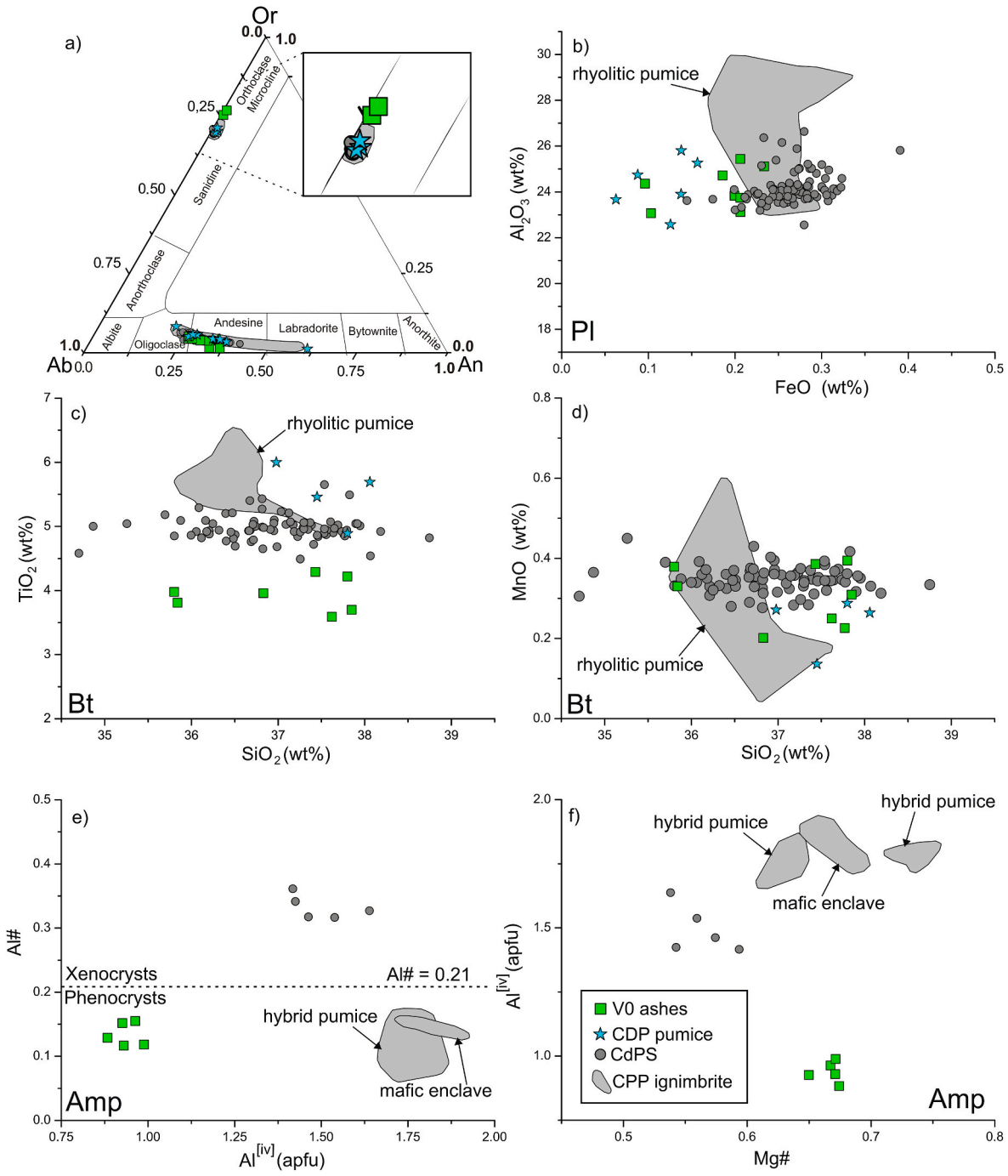

Fig. 7. Comparison of the V0 ashes with the CdPS ash samples (as in Fig. 6) considering the mineral chemistry data. We also include data from the CPP ignimbrite (Bardelli et al., 2020), including rhyolitic pumice, hybrid pumices and mafic enclaves (the last two volumetrically less important). a) Ternary diagram of feldspars (anorthite-albite-orthoclase). b) Binary diagram of Al2O3 versus FeO (wt%) for plagioclase. c) Binary diagram of TiO2 versus SiO2 and (d) MnO versus SiO2 for the biotite. e) Binary diagram of the alumina number (Al# = Al[vi]/Al[vi]+Al[iv]; following Ridolfi et al., 2010) versus Al[iv] (apfu) for the amphibole. f) Binary diagram of Al[iv] (apfu) versus Mg# [being Mg# = Mg/(g + Fe2+)] for the amphibole. Pl = plagioclase; Bt = biotite; Amp = amphibole.

stratigraphy in order to better test this hypothesis.

On the other hand, we also note that the CdPS (including our CDP sample) appear well correlated with the CPP eruption especially considering the composition of feldspars and biotite (Figs. 6 and 7). The CPP consisted in a large caldera-forming eruption (≥ VEI 6) that occurred ~54 Ka years ago and was characterized by an important initial Plinian phase (Báez et al., 2020b; de Silva et al., 2022). Fernández Turiel et al. (2019) and Bertea et al. (2021) describe pyroclastic deposits cropping out in the vicinity of the Cueros de Purulla volcano (proximal CdPS), linking them with an explosive phase of this mostly effusive volcano. However, this correlation is based solely on its spatial distribution and some litho-facial features, but lacks strong geochronological and geochemical evidences. In fact, bulk rock geochemistry of these pyroclastic deposits resembles the CPP products and differs slightly from all lavas derived from the Cueros de Purulla volcano Bertea et al. (2021). Thus, we propose that the CdPS is probably related with the CPP eruption rather than with an explosive phase of the Cueros de Purulla volcano. The comparison of glass composition of the CdPS and Cerro Paranilla ash (Fig. 6) reinforces its possible correlations as proposed by Fernández Turiel et al. (2019). In addition, Hermanns and

Schellenberger (2008) suggest that the TiO_2 content of the biotite (~5%) is a good fingerprint for the Cerro Paranilla ash. Our data from sample CDP and the available data for CdPS (Fernández Turiel et al., 2019) fit well with this fingerprint (Fig. 7c). The Holocene age constraint of the CdPS and the Cerro Paranilla ash is quite doubtful and a Pleistocene age for this tephra cannot be ruled out (Hermanns and Schellenberger, 2008), making its correlation with the CPP eruption plausible. We noted that other Upper Pleistocene tephras cropping out in the Santa María and Lerma valleys probably also correlate with this eruption (e.g., Tuff B from Malamud et al., 1996; Vp from Sampietro Vattuone et al., 2020b).

The V1a and V1b tephras are quite similar, and their geochemical fingerprints, along with their age, fit with the eruptive products of the Holocene activity of the CBVC (Figs. 8 and 9, Fernández Turiel et al., 2019; Sampietro Vattuone et al., 2020a). The morpho-stratigraphic and geochronological data indicate that the V1a and V1b tephras represent two independent explosive eruptions, likely originating from the same source (Sampietro Vattuone et al., 2020a). Our data suggest that some specific fingerprint could be used to identify and correlate both tephras, especially plagioclase and glass composition (Figs. 4 and 5). However, both tephras are practically identical from a geochemical point of view. At the current state of knowledge, the mid-Holocene activity in the CBVC includes the ~4.2 Ka caldera-forming Cerro Blanco eruption, and the pre- and post-collapse effusive activity, along with associated block and ash flows (Báez et al., 2015, 2017; 2020a; Fernández-Turiel et al., 2019).

All products of the Holocene activity of the CBVC have very homogeneous compositions (Figs. 8 and 9; Bardelli et al., 2022; de Silva et al., 2022). The well-constrained age of the V1a tephra suggests its correlation with the climactic ~4.2 caldera-forming Cerro Blanco eruption. However, to date, a major explosive event following the 4.2 Ka Plinian eruption has not been identified in the proximal zone. Usually, the superposition of constructive and destructive processes during protected volcanic activity produces a complex stratigraphic setting in proximal zones. In contrast, medial distal zones have the ability to better record the tephrochronological history of a volcanic system (Lowe, 2011). Thus, we propose that the V1b tephra identified in Tafi Valley represents an, as of yet, unidentified explosive eruption that occurred ~3500 BP following the climactic Cerro Blanco event. Further, more detailed stratigraphic studies focused on the Holocene of the CBVC are required to test this hypothesis.

The glass shard and mineral composition (especially amphibole) of the V2 tephra (Fig. 10) fit perfectly with the BdFS (Fernández Turiel et al., 2019) and the Villa Vil ash (Hermanns and Schellenberger, 2008). The V2 tephra in Tafí valley has a well-constrained age (700-650 BP) consistent with the available geochronological data for the Villa Vil ash (>980 BP, Hermanns and Schellenberger, 2008) and the BdFS (<1300 BP, Ratto, 2013; Fernández Turiel et al., 2019). Thus, we conclude that the three units represent the same tephra deposited during the Upper Holocene. Glass and mineral composition data of the "El Paso 3 ash", cropping out in the Santa Maria valley, are needed to discuss the possible existence of a tephra similar to V2 but slightly younger (<400 BP, Sampietro Vattuone et al., 2018a, 2020a). The geochemical features of the V2 tephra suggest a dacitic composition more compatible with the typical stratovolcanoes of the main arc, rather than the rhyolitic CBVC (Fernández Turiel et al., 2019; Sampietro Vattuone et al., 2020a). Previous works proposed that the strongest candidate to be the source of V2

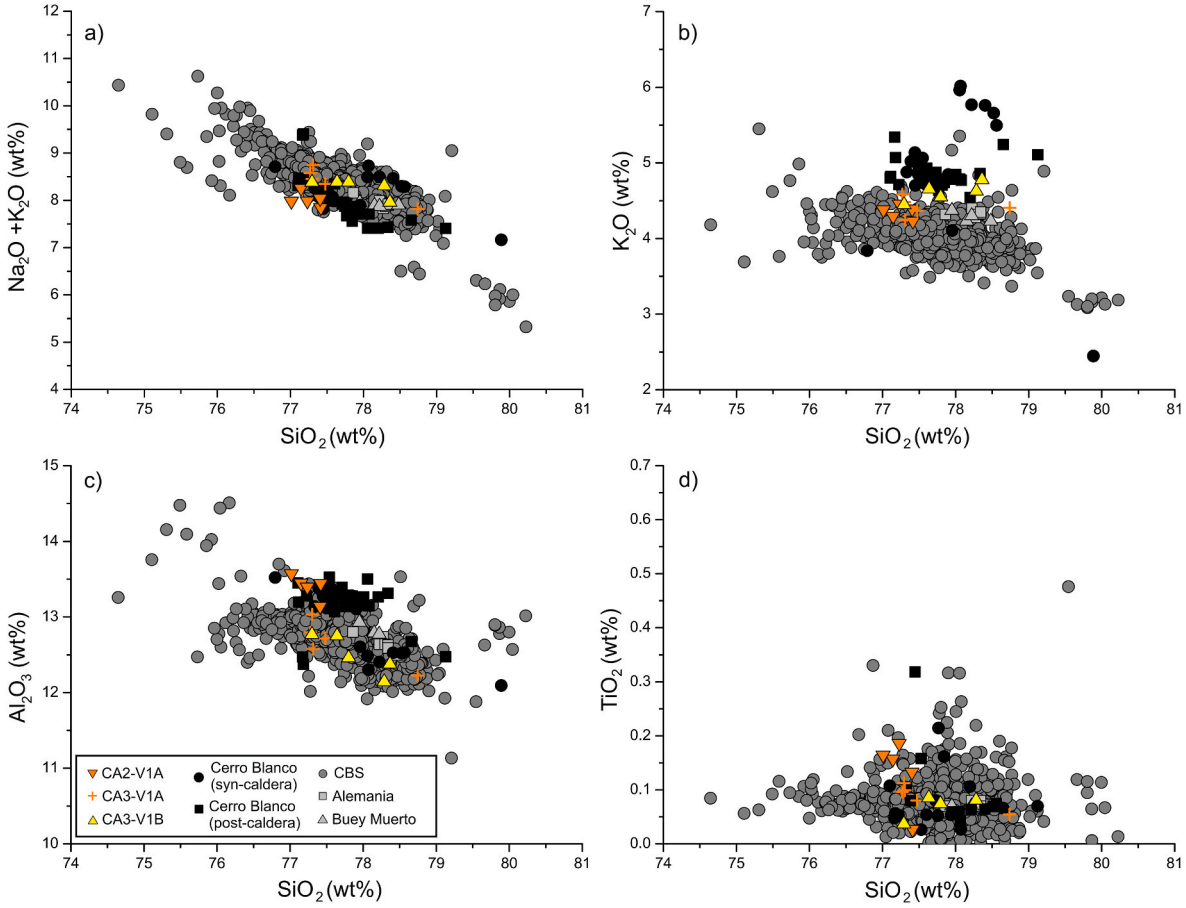

Fig. 8. Comparison of the V1 ashes with (i) the CBS ash samples of Fernandéz-Turiel et al. (2019, and references therein), (ii) the Cerro Blanco syn-caldera and post-caldera products (Bardelli et al., 2022), and (iii) the Alemania/Buey Muerto ash samples (average composition) following (Hermanns and Schellenberger, 2008). a) Na2O + K2O versus SiO2. b) K2O versus SiO2. c) Al2O3 versus SiO2. d) TiO2 versus SiO2.

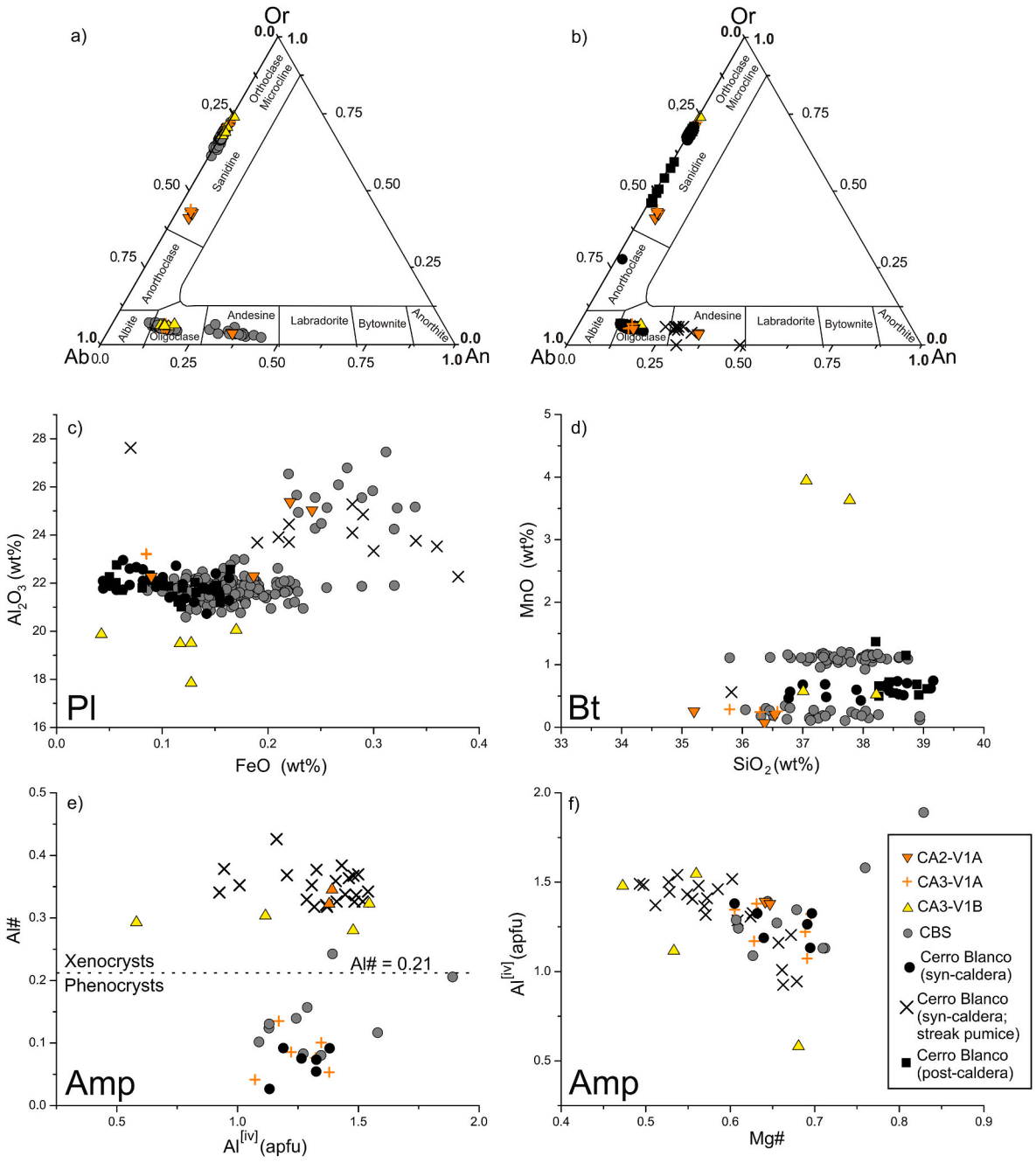

Fig. 9. Comparison of the V1 ashes (as in Fig. 8) considering the mineral chemistry data. a-b) Ternary diagram of feldspars (anorthite-albite-orthoclase). c) Binary diagram of Al2O3 versus FeO (wt%) for plagioclase. d) Binary diagram of MnO versus SiO2 for the biotite. e) Binary diagram of the alumina number (Al# = Al[vi]/Al[vi]+Al[iv]; following Ridolfi et al., 2010) versus Al[iv] (apfu) for the amphibole. f) Binary diagram of Al[iv] (apfu) versus Mg# [being Mg# = Mg/(g + Fe2+)] for the amphibole. Pl = plagioclase; Bt = biotite; Amp = amphibole.

tephra is the Nevado Tres Cruces volcano (Fernández Turiel et al., 2019; Sampietro Vattuone et al., 2020a).

In fact, the Nevado Tres Cruces volcano recorded an important explosive eruption which produced large amounts of PDCs and plinian fall-out deposits (Gardeweg et al., 2000). However, this explosive eruption occurred during the Upper Pleistocene (~67 Ka, Gardeweg et al., 2000), thus its correlation with V2 is unlikely. The region of the Nevado Tres Cruces Volcano hosts many potentially active volcanoes (e.g., Incahuasi, Ojos del Salado, El Fraile, Tipas, Peinado) and is considered a volcanic cluster with a high spatial probability of future volcanic activity (Fig. 1b; Incahuasi cluster, Bertin et al., 2022). In this sense, the spatial distribution of the V2 (Taff valley, Villa Vil, Bolson de Fiambalá; Fig. 1) tephra as well as its geochemical composition, suggests that its source is likely within the Incahuasi cluster, but the specific eruptive center remains unknown. For instance, some studies mentioned the occurrence of a major rhyodacitic explosive eruption at about 1000–1500 years ago in the Ojos del Salado volcano (Global Volcanism Program, 2023). Despite the fact that the age of this eruption appears to be consistent with the age of V2, the information about this event is very scarce, preventing any attempt of a reliable correlation. High-resolution studies on the Incahuasi cluster are needed to achieve a final identification of the emission center of the V2 tephra.

6. Conclusions

Our characterization of glass shards and minerals from the Holocene

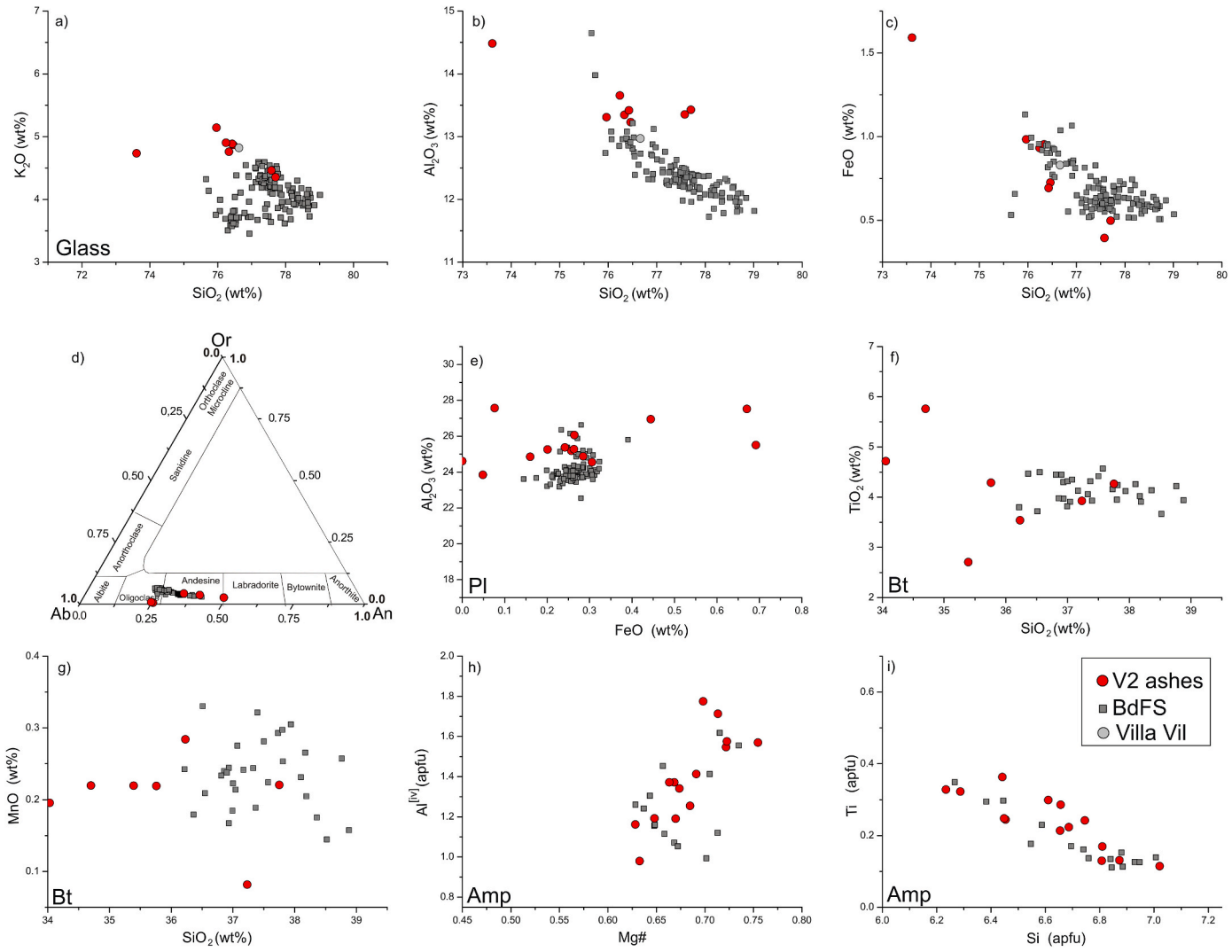

Fig. 10. Comparison with V2 ashes with (i) the BdfS ash samples from Fernandéz-Turiel et al. (2019) and (ii) the Villa Vil ash samples (average composition) following (Hermanns and Schellenberger, 2008), considering both glass and mineral chemistry data. a-c) Binary diagrams of K2O (a), Al2O3 (b) and FeO (c) versus SiO2 for the volcanic glass. d) Ternary diagram of feldspars (anorthite-albite-orthoclase). e) Binary diagram of Al2O3 versus FeO (wt%) for plagioclase. f) Binary diagram of TiO2 versus SiO2 and (g) MnO versus SiO2 for the biotite. h) Binary diagram of Al[iv] (apfu) versus Mg# [being Mg# = Mg/(g + Fe2+)] and (i) of cationic Ti versus Si (apfu) for the amphibole. Pl = plagioclase; Bt = biotite; Amp = amphibole.

tephras cropping out in the Taff valley (V0, V1a, V1b and V2) reveals the existence of well-constrained geochemical fingerprints for most of them. However, distinguishing between V1a and V1b remains challenging using glass and mineral composition. The identified fingerprint allows for the correlation of the four tephras on a regional scale (NW Argentina). Thus, we present a revised Holocene tephrochronological scheme for NW Argentina. Our data also allowed us to discuss the possible source of each tephra. The V0 tephra does not derive from the Cueros de Purulla volcano, as previously postulated. Considering the Holocene age and the main geochemical features of the V0 tephra, the strongest candidate for their source is the CBVC. Thus, the V0 tephra probably represents a not identified explosive eruption occurred during the Lower Holocene in the CBVC. In addition, the previously defined "CdPS" could have an Upper Pleistocene age and correlates with the Campo de la Piedra Pómez eruption (CBVC). The V1a tephra correlate with the ~4.2 Ka caldera-forming Cerro Blanco eruption (CBVC). The V1b likely represents an unknown explosive event of the CBVC, occurred ~3.5 Ka, which followed the climatic Cerro Blanco eruption. The Upper Holocene V2 tephra (~700-650 BP) likely derives from the main arc, specifically from the Incahuasi cluster. However, the exact source of the V2 tephra remains unknown.

We highlight that a more robust geochemical database (glass and mineral geochemistry) of the Holocene tephras of NW Argentina, along with a better knowledge of the volcanic centers considered as sources, is necessary to achieve an ultimate tephrochronology framework for this region. Even so, our work is a valuable upgrade of the Holocene tephrochronology of NW Argentina. In addition, the identification of three remarkable Holocene explosive eruptions in the CBVC (plus another large eruption during Upper Pleistocene) make this volcanic system one of the most worrisome for NW Argentina in terms of hazard and risk, especially due to dispersion and ash fall. Lastly, the occurrence of a massive eruption in the Incahuasi cluster dating back to approximately 700-650 years BP, confirmed by the regional correlation of the V2 tephra, reinforces the claim that this area holds one of the highest spatial probabilities of future volcanic activity along the Central Andes.

CRediT authorship contribution statement

W. Báez: Writing - original draft, Investigation, Funding acquisition, Formal analysis, Data curation, Conceptualization. **L. Bardelli:** Writing - review & editing, Visualization, Formal analysis, Data curation. **M.M. Sampietro-Vattuone:** Writing - review & editing, Visualization,

Validation, Data curation. **J.L. Peña Monné:** Writing - review & editing, Visualization, Validation, Formal analysis, Data curation. **E. Bertea:** Writing - review & editing, Validation, Investigation. **M. Cirer:** Writing - review & editing, Validation, Investigation.

Declaration of competing interest

The authors declare that they have no known competing financial interests or personal relationships that could have appeared to influence the work reported in this paper.

Data availability

Data will be made available on request.

Acknowledgments

This research was supported by the grants PICT-2018-01350, PICT2018-1119 and PICT2019-0193; from Agencia Nacional de Promoción Científica y Tecnológica (Argentina).We warmly thank the team of the "*Laboratorio de Microscopía Electrónica y Análisis por Rayos X*" (LAMARX) of the National University of Córdoba (Argentina) for their support during the EMPA analyses. We thoroughly appreciate the thoughtful reviews by the Editor-in-Chief Andres Folguera and an anonymous reviewer. Their comments and concerns have helped us focus and improve our work significantly.

Appendix A. Supplementary data

Supplementary data to this article can be found online at https://doi.org/10.1016/j.jsames.2023.104745.

References

Aguilera, F., Apaza, F., Del Carpio, J., Grosse, P., Jiménez, N., Ureta, G., Inostroza, M., Báez, W., Layana, S., Gonzalez, C., Rivera, M., Ortega, M., Gonzalez, R., Iriarte, R., 2022. Advances in scientific understanding of the Central Volcanic Zone of the Andes: a review of contributing factors. Bull. Volcanol. 84 (3), 22.

Amigo, A., Bertin, D., Orozco, G., 2012. Peligros volcánicos de la zona norte de Chile. In: Servicio Nacional de Geología y Minería, Chile (Santiago, Chile, vol. 17. Servicio Nacional de Geología y Minería), p. 45 *(Serie Geología Ambiental*.

Báez, W., Arnosio, M., Chiodi, A., Ortiz Yañes, A., Viramonte, J.G., Bustos, E., Giordano, G., López, J.F., 2015. Estratigrafía y evolución del Complejo Volcánico Cerro Blanco, Puna Austral, Argentina. Rev. Mex. Ciencias Geol. 32 (1), 29–49.

Báez, W.A., Chiodi, A.L., Bustos, E., Arnosio, J.M., Viramonte, J.G., Giordano, G., Alfaro Ortega, B.B., 2017. Mecanismos de emplazamiento y destrucción de los domos lávicos asociados a la caldera del Cerro Blanco, Puna Austral.

Báez, W., Bustos, E., Chiodi, A., Reckziegel, F., Arnosio, M., de Silva, S., Giordano, G., Viramonte, J.G., Sampietro-Vattuone, M.M., Peña-Monné, J.L., 2020a. Eruptive style and flow dynamics of the pyroclastic density currents related to the Holocene Cerro Blanco eruption (Southern Puna plateau, Argentina). J. S. Am. Earth Sci. 98, 102482.

Báez, W., de Silva, S., Chiodi, A., Bustos, E., Giordano, G., Arnosio, M., Suzaño, N., Viramonte, J.G., Norini, G., Groppelli, G., 2020b. Pulsating flow dynamics of sustained, forced pyroclastic density currents: insights from a facies analysis of the Campo de la Piedra Pómez ignimbrite, southern Puna, Argentina. Bull. Volcanol. 82, 1–32.

Báez, W., Bustos, E., Chiodi, A., García, H.P.A., Álvarez, O., Simón, V., Folguera, A., 2023. Reviewing the geodynamic impact of aseismic ridges subduction on the tectonic-magmatic evolution of the Southern Puna plateau. J. S. Am. Earth Sci. 104520.

Bardelli, L., Arnosio, M., Báez, W., Suzaño, N., Becchio, R., Viramonte, J.G., Bustos, E., Bertea, E., 2020. Multi-banded pumice in the Campo de la Piedra Pómez rhyolitic ignimbrite (Southern Puna plateau): pre-eruptive physical and chemical interaction between mafic and rhyolitic melts. J. S. Am. Earth Sci. 101 (2), 102616.

Bardelli, L., Lucci, F., Arnosio, M., Bustos, E., Becchio, R., Filipovich, R., Villagrán, A., Viramonte, J.G., 2022. The rise and fate of a long-lived deep crustal "hot zone" beneath the neogene-quaternary Cordillera de San Buenaventura in the Southern Puna plateau (NW Argentina). Int. Geol. Rev.65:15, 2447-2478.

Bertea, E.S., Báez, W., Bustos, E., Filipovich, R.E., Bardelli, L., Arnosio, M., Villagrán, A., Sommer, C.A., Alfaro Ortega, B., Chiodi, A., 2021. Cartografía y reconstrucción de la historia eruptiva del Volcán Cueros de Purulla, Puna Austral, Provincia de Catamarca. Rev. Asoc. Geol. Argent. 78 (2), 284–310.

Bertin, D., Lindsay, J.M., Cronin, S.J., de Silva, S.L., Connor, C.B., Caffe, P.J., Grosse, P., Báez, W., Bustos, E., Constantinescu, R., 2022. Probabilistic volcanic hazard assessment of the 22.5–28°S Segment of the central volcanic zone of the Andes. Front. Earth Sci. 10, 875439.

Bertin, D., de Silva, S., Lindsay, J., Cronin, S., Caffe, P., Connor, c., Grosse, P., Báez, W., Bustos, E., Constantinescu, R., 2023. Magmatic addition rates differentiate periods of steadystate versus flare-up magmatism in the Central Andean arc. Communications Earth & Environment 4 (1), 75.

Bolli, M.I., 1996. Estudio geologico de los Depósitos de Tefra en el Cuaternario de los Valles de Lerma y Sianca – Provincia de Salta. Universidad Nacional de Salta. *Unpublished degree thesis*.

Boretto, G., Zanchetta, G., Bini, M., Cioccale, M., Carignano, C., Gordillo, S., Giaccio, B., Fernández Turiel, J.L., Arienzo, I., Isola, I., 2021. Cerro Blanco 4.2 Ka Volcanic Ash Deposit at Cerro Colorado (Córdoba Province, Argentina).

Carbonelli, J.P., Fernandez-Turiel, J.L., de Medina, C.B.L., 2022. The Abra del Toro rock shelter, northwestern Argentina, a space occupied by hunter-gatherers that was hit by the large 4.2 ka Cerro Blanco eruption. J. Archaeol. Sci.: Reports 45, 103629.

Coira, B., Galli, C.I., Mahlburg Kay, S., Kay, R.W., Flores, P., 2014. Niveles piroclásticos como herramientas de correlación en los depósitos cenozoicos del Grupo Payogastilla, Valles Calchaquí, Tonco y Amblayo, en el noroeste de Argentina. Rev. Asoc. Geol. Argent. 71 (2), 147–160.

Coira, B., Galli, C.I., Kay, S.M., Alonso, R.N., Flores, P., González, E.D., 2022a. Cenozoic ash-fall deposits in the Andean foreland basins, Northwest Argentina (23°-26° S)-Key to reconstruct their chrono-stratigraphy and to identify links to the Andean Neogene ignimbrite flare-up. J. S. Am. Earth Sci. 116, 103792.

Coira, B., Galli, C.I., Mahlburg-Kay, S., Stockli, D.F., Flores, P., Eveling, E., 2022b. Pliocene-Pleistocene ash-fall tuff deposits in the intermountain Humahuaca and Casa Grande basins, northwestern Argentina: tracers in chronostratigraphic reconstructions and key to identify their volcanic sources. Andean Geol. 49 (2), 208–237.

Collantes, M.M., 2007. Evolución morfogenética y paleoambiental del valle de Tafí durante el Pleistoceno tardío y Holoceno. In: Arenas, P., Manasse, B., Noli, E. (Eds.), Paisajes y procesos sociales en Tafí del Valle. Magna Publicaciones, Tucumán Argentina, pp. 261–288.

de Silva, S.L., y Francis, P., 1991. Volcanoes of the Central Andes, vol. 220. Springer-Verlag, Berlin.

de Silva, S.L., Roberge, J., Bardelli, L., Báez, W., Ortiz, A., Viramonte, J.G., Arnosio, M., Becchio, R., 2022. Magmatic evolution and architecture of an arc-related, rhyolitic caldera complex: the late Pleistocene to Holocene Cerro Blanco volcanic complex, southern Puna, Argentina. Geosphere 18 (2), 394–423.

Donovan, A., Toyos, G., Amigo, A., Villarosa, G., Lafranco, G.O., Rovere, E., 2023. Managing cross-border eruptions: insights from recent crises in Chile and Argentina. J. Volcanol. Geoth. Res. 107774.

Dzierma, Y., Wehrmann, H., 2012. On the likelihood of future eruptions in the Chilean Southern Volcanic Zone: interpreting the past century's eruption record based on statistical analyses. Andean Geol. 39 (3), 380–393.

Elissondo, M., Farias, C., Collini, E., 2017. Evaluación del riesgo volcánico relativo en Argentina. Simposio 10 III simposio sobre volcanes activos. In: XX Congreso Geológico Argentino, pp. 36–38. Actas.

Fernández-Turiel, J.L., Perez-Torrado, F.J., Rodríguez González, A., Saavedra, J., Carracedo, J.C., Rejas, M., Lobo, A., Osterrieth, M., Carrizo, J., Esteban, G., Gallardo, J., Ratto, N., 2019. The large eruption 4.2 ka cal BP in Cerro Blanco, central volcanic zone, Andes: insights to the Holocene eruptive deposits in the southern Puna and adjacent regions. Estud. Geol. 718 (1), 75.

Forte, P., Ramires, A., De Abrantes, L., Llano, J., Dominguez, L., Carbajal, F., García, S., Sruoga, P., Bonadonna, C., 2022. La erupción no será transmitida: características, impactos y asistencia durante el ciclo eruptivo 2018-2019 del volcán Peteroa, Argentina. Rev. Asoc. Geol. Argent. 79 (1), 47–71.

Frenguelli, J., 1936. Investigaciones geológicas en la zona salteña del valle de Santa María. Obra del Cincuentenario del Museo de La Plata. In: Obra del Cincuentenario del Museo de La Plata, pp. 215–572. La Plata.

Galván, A.F., 1981. Descripción geológica de la Hoja 10e, Cafayate, Provincias de Tucumán, Salta y Catamarca. Escala 1:200.000. In: Servicio Geológico Nacional, Boletín 177. Servicio Geológico Nacional, Buenos Aires, Argentina.

Gardeweg, M.C., Sparks, R.S.J., Matthews, S.J., 1998. Evolution of Lascar volcano, northern Chile. J. Geol. Soc. 155 (1), 89–104.

Gardeweg, M., Clavero, J., Mpodozis, C., Pérezde, A.C., Villeneuve, M., 2000. El Macizo Tres Cruces: un complejo volcánico longevo y potencialmente activo en la Alta Cordillera de Copiapó, Chile. In: Actas IX Congreso Geológico Chileno, Simposio Geología y Recursos Minerales de los Andes Centrales, avances del Proyecto Multinacional Andino, MAP, pp. 291–295.

Garreaud, R.D., Vuille, M., Compagnucci, R., Marengo, J., 2009. Present-day South American climate. Palaeogeogr. Palaeoclimatol. Palaeoecol. 281, 180–195.

Global Volcanism Program, 2023. [Database] Volcanoes of the World (V. 5.1.1; 17 Aug 2023. E. *Distributed by Smithsonian Institution, compiled by Venzke*.

González, O.E., 1997. Geología de La Angostura, valle de Tafí, Tucuman. In: XIV Congreso Geológico Argentino. Salta, Argentina, pp. 283–286.

Guerra, L., Martini, M.A., Vogel, H., Piovano, E.L., Hajdas, I., Astini, R., De Haller, A., Moscariello, A., Loizeau, J., Ariztegui, D., 2022. Microstratigraphy and palaeoenvironmental implications of a Late Quaternary high-altitude lacustrine record in the subtropical Andes. Sedimentology 69 (6), 2585–2614.

Guzmán, S., Grosse, P., Montero-López, C., Hongn, F., Pilger, R., Petrinovic, I., Seggiaro, A., Aramayo, A., 2014. Spatial–temporal distribution of explosive volcanism in the 25–28 S segment of the Andean Central Volcanic Zone: Tectonophysics 636, 170–189.

Hain, M.P., Strecker, M.R., Bookhagen, B., Alonso, R.N., Pingel, H., Schmitt, 2011. Neogene to Quaternary broken foreland formation and sedimentation dynamics in the Andes of NW Argentina (25 S). Tectonics 30 (2).

Hansell, A.L., Horwell, C.J., Oppenheimer, C., 2006. The health hazards of volcanoes and geothermal areas. Occup. Environ. Med. 63 (2), 149–156.

Hermanns, R.L., Schellenberger, A., 2008. Quaternary tephrochronology helps define conditioning factors and triggering mechanisms of rock avalanches in NW Argentina. Quat. Int. 178, 261–275.
Hermanns, R.L., Trauth, M.H., Niedermann, S., McWilliams, M., Strecker, M.R., 2000. Tephrochronologic constraints on temporal distribution of large landslides in northwest Argentina. J. Geol. 108, 35–52.
Hurst, T., Smith, W., 2004. A Monte Carlo methodology for modelling ashfall hazards. J. Volcanol. Geoth. Res. 138, 393e403.
Hurst, T., Smith, W., 2010. Volcanic ashfall in New Zealand e probabilistic hazard modelling for multiple sources. N. Z. J. Geol. Geophys. 53, 1e14.
Jenkins, S.F., Magill, C.R., McAneney, K.J., 2007. Multi-stage volcanic events: a statistical investigation. J. Volcanol. Geoth. Res. 161, 275e288.
Jenkins, S.F., Wilson, T.M., Magill, C., Miller, V., Stewart, C., Blong, R., Marzocchi, W., Boulton, M., Bonadonna, C., Costa, A., 2015. Volcanic ash fall hazard and risk. Global volcanic hazards and risk 173–222.
Kay, S.M., Coira, B.L., 2009. Shallowing and steepening subduction zones, continental lithospheric loss, magmatism, and crustal flow under the Central Andean Altiplano-Puna Plateau. Backbone of the Americas: Shallow Subduction, Plateau Uplift, and Ridge and Terrane Collision, Suzanne Mahlburg Kay. William R. Dickinson. Víctor A. Ramos.
Lara, L.E., Orozco, G., Amigo, A., Silva, C., 2011. Peligros volcánicos de Chile. Servicio Nacional de Geología y Minería, Carta Geológica de Chile. Serie Geología Ambiental (Santiago, Chile: Sernageomin) 13, 34. *1 mapa escala 1:2.000.000*.
Li, X., Zhang, C., Behrens, H., Holtz, F., 2020. Calculating biotite formula from electron microprobe analyses data using a machine learning method based on principal components regression. Lithos 356–357, 105371.
Lindsay, J., Marzocchi, W., Jolly, G., Constantinescu, R., Selva, J., Sandri, L., 2009. Towards real-time eruption forecasting in the Auckland volcanic field: application of BET_EF during the New Zealand National Disaster exercise 'Ruaumoko'. Bull. Volcanol. 72, 185e204.
Locock, A.J., 2014. An Excel spreadsheet to classify chemical analyses of amphiboles following the IMA 2012 recommendations. Comput. Geosci. 62, 1–11.
Lowe, D.J., 2011. Tephrochronology and its application: a review. Quat. Geochronol. 6 (2), 107–153.
Lucci, F., Carrasco-Núnez, G., Rossetti, F., Theye, T., White, J.C., Urbani, S., Azizi, H., Asahara, Y., Giordano, G., 2020. Anatomy of the magmatic plumbing system of Los Humeros Caldera (Mexico): implications for geothermal systems. Solid Earth 11, 125–159.
Malamud, B.D., Jordan, T.E., Alonso, R.A., Gallardo, E.F., González, R.E., Kelley, S.A., 1996. Pleistocene Lake Lerma, Salta Province, NW Argentina. In: 18° Congreso Geológico Argentino y 3° Congreso de Exploración de Hidrocarburos, pp. 103–114. Actas.
Montero-López, M.C., 2009. Estructura y magmatismo neógeno-cuaternarios en la sierra de San Buenaventura (Catamarca): su vinculación con la terminación austral de la Puna. Ph.D. Thesis. Salta University.
Montero-López, M.C., Hongn, F.D., Seggiaro, R., Marrett, R., Ratto, N., 2009. In: en Ratto, N. (Ed.), Relación entre el volcanismo y los registros arqueológicos en el bolsón de Fiambalá, Entrelazando ciencias, sociedad y ambiente antes de la conquista española: Buenos Aires. Editorial Eudeba, pp. 131–156.
Montero-López, M.C., Hongn, F., Brod, J.A., Seggiaro, R., Marrett, R., Sudo, M., 2010. Magmatismo ácido del Mioceno Superior-Cuaternario en el área de Cerro Blanco- La Hoyada, Puna Austral. Rev. Asoc. Geol. Argent. 67, 329–348.
Peccerillo, A., Taylor, S.R., 1976. Geochemistry of Eocene calc-alkaline volcanic rocks from the Kastamonu area, Northern Turkey. Contribution to Mineralogy and Petrology 58, 63–81.
Peña Monné, J.L., Sampietro Vattuone, M.M., 2016. La secuencia paleoambiental holocena de la vertiente oriental de Loma Pelada (valle de Tafí, Noroeste Argentino): cambios climáticos y acción humana. In: Sampietro Vattuone, M.M., Peña Monné, J. L. (Eds.), Geoarqueología de los Valles Calchaquíes. Laboratorio de Geoarqueología, Tucumán, Argentina, pp. 23–63.
Peña-Monné, J.L., Sampietro-Vattuone, M.M., 2019. Late Holocene anthropic degradation records in semi-arid environments (NE Spain and NW Argentina). Cuadernos de Investigación Geográfica 45 (1), 195–217.
Petrinovic, I.A., Grosse, P., Guzmán, S., Caffe, P.J., 2017. Evolución del volcanismo Cenozoico en la Puna Argentina.
Ratto, N., 2013. A modo de introducción: la articulación de estudios arqueológicos, paleoambientales e históricos en el oeste tinogasteño (Catamarca). In: Ratto, N. (Ed.), Delineando prácticas de la gente del pasado: Los procesos socio-históricos del oeste catamarqueño. Sociedad Argentina de Antropología, Buenos Aires, pp. 17–44.
Retamoso, S., Ramos, P., Elías, L., Leguizamón, E., Ruiz, P., Báez, W., 2021. Evidencia de resedimentación y análisis de flujo de los niveles de cenizas de la Formación La Viña, Valle de Lerma, Salta. XVII RAS y del VIII CLS. Entre Ríos, Argentina. *October 2021, Paraná*.
Ridolfi, F., Renzulli, A., Puerini, M., 2010. Stability and chemical equilibrium of amphibole in calc-alkaline magmas: an overview, new thermobarometric formulations and application to subduction-related volcanoes: Contributions to Mineralogy and Petrology 160, 45–66.
Ridolfi, F., Zanetti, A., Renzulli, A., Perugini, D., Holtz, F., Oberti, R., 2018. AMFORM, a new mass-based model for the calculation of the unit formula of amphiboles from electron microprobe analyses. Am. Mineral. 103, 1112–1125.
Rieder, M., Cavazzini, G., D'yakonov, Y.S., Frank-Kamenetskii, V.A., Gottardi, G., Guggenheim, S., Koval, P.V., Mueller, G., Neiva, A.M.R., Radoslovich, E.W., Robert, J.-L., Sassi, F.P., Takeda, H., Weiss, Z., Wones, D.R., 1998. Nomenclature of the micas. Clay Clay Miner. 46, 586–595.
Ruiz Huidobro, O.J., 1972. Descripción Geológica de la hoja 11e, Santa María, Provincias de Catamarca y Tucumán. Servicio Nacional Minero Geológico, Boletín 134. Servicio Nacional Minero Geológico, Buenos Aires, Argentina.
Sampietro Vattuone, M.M., Peña Monné, J.L., Báez, W., Ortíz, P., Aguirre, M.G., 2016. Unidades morfosedimentarias holocenas en la quebrada de La Angostura (Valle de Tafí, Noroeste Argentino). In: Sampietro Vattuone, M.M., Peña Monné, J.L. (Eds.), Geoarqueología de los Valles Calchaquíes. Laboratorio de Geoarqueología, Universidad Nacional de Tucumán, pp. 3–22. ISBN 978-987-42-0568-1.
Sampietro Vattuone, M.M., Peña-Monné, J.L., Roldán, J., Maldonado, M.G., Lefebvre, M. G., Vattuone, M.A., 2018b. Human-driven geomorphological processes and soil degradation in Northwest Argentina: a geoarchaeological view. Land Degrad. Dev. 29, 3852–3865.
Sampietro-Vattuone, M.M., Peña-Monné, J.L., 2016. Geomorphological dynamic changes during the Holocene through ephemeral stream analyses from Northwest Argentina. Catena 147, 663–677.
Sampietro-Vattuone, M.M., Peña-Monné, J.L., 2019. Geomorphology of Tafí valley (Tucumán Province, northwest Argentina). J. Maps 15 (2), 177–184.
Sampietro-Vattuone, M.M., Sola, A., Báez, W., Peña Monné, J.L., 2017. Aplicación de la correlación geoquímica de niveles cineríticos en la reconstrucción de las secuencias morfosedimentarias holocenas del valle de Tafí. XX. Congreso Geológico Argentino, Tucumán, 2017.
Sampietro-Vattuone, M.M., Peña Monné, J.L., Maldonado, M.G., Marcén, C.S., Báez, W., Sola, A., Blasi, A., 2018a. Cambios ambientales durante el Holoceno superior registrados en secuencias morfosedimentarias fluvio-eólicas del Valle de Santa María (Noroeste Argentino). Bol. Geol. Min. 129 (4), 647–669.
Sampietro-Vattuone, M.M., Báez, W., Peña-Monné, J.L., Sola, A., 2020a. Chronological and geomorphological approach to the Holocene tephras from Tafí and Santa María valleys, NWArgentina. Quat. Res. 94, 14–30.
Sampietro-Vattuone, M.M., Peña-Monné, J.L., Báez, W., Sola, A., Somonte, C., 2020b. Geomorphological and chronostratigraphical context of the La Sala lithic artifacts (Amaicha basin - northwest Argentina). J. Archaeol. Sci.: Reports 29, 102168.
Shane, P.A.R., Hoverd, J., 2002. Distal record of multi-sourced tephra in Onepoto Basin, Auckland, New Zealand: implications for volcanic chronology, frequency and hazards. Bull. Volcanol. 64, 441e454.
Siebel, W., Schnurr, W.B., Hahne, K., Kraemer, B., Trumbull, R.B., van den Bogaard, P., Emmermann, R., 2001. Geochemistry and isotope systematics of small-to medium-volume Neogene–Quaternary ignimbrites in the southern central Andes: evidence for derivation from andesitic magma sources. Chem. Geol. 171 (3–4), 213–237.
Sola, A.M., Báez, W., Bustos, E., Hernandez, R., Sampietro Vattuone, M.M., Peña Monné, J.L., Becchio, R.A., 2016. Cluster analysis using portable X ray fluorescence (pXRF) data: a fast and powerful method for regional correlation of ash fall deposits. In: Actas del Cities on Volcanoes 9, Puerto Varas, Chile, vol. 25, p. 2016. November 20 to.
Sola, A., Báez, W., Sánchez, M.C., Díaz Trigo, S., 2018. Caracterización geoquímica y correlación de las tobas cuaternarias aflorantes en el Valle del Tonco, provincia de Salta. Actas de la XVI Reunión Argentina de Sedimentología, November. General Roca, Río Negro, p. 83.
Strecker, M.R., 1987. Late Cenozoic Landscape Development, the Santa María Valley, Northwest Argentina. PhD Dissertation. Cornell University, Ithaca, NY.
Toselli, A.J., Rossi de Toselli, J.N., Rapela, C.W., 1978. El basamento metamórfico de la Sierra de Quilmes, República Argentina. Rev. Asoc. Geol. Argent. 33, 105–121.
Trauth, M.H., Bookhagen, B., Marwan, N., Strecker, M.R., 2003. Multiple landslide clusters record Quaternary climate changes in the northwestern Argentine Andes. Palaeogeogr. Palaeoclimatol. Palaeoecol. 194 (1–3), 109–121.
Trumbull, R.B., Riller, U., Oncken, O., Scheuber, E., Munier, K., Hongn, F., 2006. The time-space distribution of Cenozoic volcanism in the South-Central Andes: a new data compilation and some tectonic implications. Andes: active subduction orogeny 29–43.
Turner, M., Cronin, S., Bebbington, M., Platz, T., 2008. Developing probabilistic eruption forecasts for dormant volcanoes: a case study from Mt Taranaki, New Zealand. Bull. Volcanol. 70, 507e515.
Turner, M.B., Bebbington, M.S., Cronin, S.J., Stewart, R.B., 2009. Merging eruption datasets: building an integrated Holocene eruptive record for Mt Taranaki, New Zealand. Bull. Volcanol. 71, 903e918.
Wörner, G., Mamani, M., Blum-Oeste, M., 2018. Magmatism in the central Andes. Elements 14 (4), 237–244.